Deanship of Graduate Studies

Al-Quds University

Channel Estimation For FBMC/OQAM Wireless System Based On Kalman Filter

Mahmoud Hassan Khaleel Aldababseh

M.Sc Thesis

Jerusalem-Palestine

1434-2013

Channel Estimation For FBMC/OQAM Wireless System Based On Kalman Filter

Prepared By:

Mahmoud Hassan Khaleel Aldababseh

B.Sc.: Electrical Engineering, 2010, Palestine

An-Najah National University, Palestine

Supervisor: Dr. Ali Jamoos

A thesis submitted in partial fulfilment of the requirements for the degree of Master of Electronic and Computer Engineering/ Faculty of Engineering/ Graduate Studies

Jerusalem-Palestine

1434-2013

Al-Quds University

Deanship of Graduate Studies

Master of Electronics and Computer Engineering

Thesis Approval

Channel Estimation For FBMC/OQAM Wireless

System Based On Kalman Filter

Prepared By: Mahmoud Hassan Khaleel Aldababseh

Registration No: 21020187

Supervisor: Dr. Ali Jamoos

Master thesis submitted and accepted, Date: 13/08/2013

The name and signatures of examining committee members are as follows:

1- Head of committee	Dr. Ali Jamoos	Signature: …………….
2- Internal Examiner	Dr. Hanna Abdel Nour	Signature: …………….
3- External Examiner	Dr. Ghandi Manasrah	Signature: …………….

Jerusalem-Palestine

1434-2013

Declaration:

I certify that this thesis submitted for the degree of Master, is the result of my own research, except where otherwise acknowledged, and that this study (or any part of the same) has not been submitted for a higher degree to any other university or institution.

Signed: ……………

Mahmoud Hassan Khaleel Aldababseh

Date: …………….

Acknowledgments

I thank God for everything.

I would like to express my deepest appreciation to my family especially my parents, for the endless care they have provided me, advices, support and patience.

Special thanks goes out to my supervisor, Dr. Ali Jamoos, who has given me more knowledge and skills in the communication field. In addition, his guidance helped me throughout this research and the writing of this thesis.

My sincere thanks also goes to Dr. Hanna Abdel Nour for helping me in topics related to digital signal processing.

My deep gratitude goes to all my friends, especially at An-Najah National University and at Al-Quds University.

I would like to express my gratitude to all those who helped me during the period of my study and gave me motivation and encouragement.

Abstract

Multicarrier (MC) modulation is an attractive technology for high data rate communication systems due in part to their robustness against long delay spread and lower complexity when compared to single carrier systems. The most widely used MC modulation technique at the time is the orthogonal frequency division multiplexing (OFDM). This technique uses the so-called cyclic prefix (CP) to solve inter-symbol interference (ISI) and inter-carrier interference (ICI) problems. Nevertheless, using the CP implies a reduction of the energy efficiency of the transmission. An alternative to OFDM, which does not require the use of CP, is the filter bank multicarrier (FBMC) modulation. The main difference between FBMC and OFDM is that instead of using a rectangular window a more advanced prototype filter is employed. This can reduce the spectral leakage problem of OFDM resulting in negligible ISI and ICI. In addition, the combination of FBMC with offset quadrature amplitude modulation (FBMC/OQAM) leads to a higher data transmission rate.

This thesis deals with the problem of fading channel estimation in FBMC/OQAM wireless systems based on pilot symbols. The standard solution to this problem is the least square (LS) estimator or the minimum mean square error (MMSE) estimator with possible adaptive implementation using recursive least square (RLS) algorithm or least mean square (LMS) algorithm. However, these adaptive filters cannot well exploit fading channel statistics. To take advantage of fading channel statistics, the evolution of the fading channel is modeled by an autoregressive (AR) process and tracked by an optimal Kalman filter. Nevertheless, this requires the autoregressive parameters which are usually unknown. Thus, we propose to jointly estimate the

FBMC/OQAM fading channels and their autoregressive parameters based on dual Kalman filters. Once the fading channel coefficients at pilot symbol positions are estimated by the proposed method, the fading channel coefficients at data symbol positions are then estimated by using some interpolation methods such as linear, spline, or low-pass interpolation. FBMC/OQAM wireless system model implemented using Matlab program and the simulation results showed that dual Kalman filters based estimator outperforms the LMS and RLS based ones. In addition, the low-pass interpolation is confirmed to outperform both spline and linear interpolation.

Keywords: FBMC/OQAM, fading channel, autoregressive model, dual Kalman Filters, LMS, RLS, pilot symbols, interpolation.

Table of Contents

List of Figures

Chapter 1

Introduction

Wireless multicarrier communication systems are parallel data transmission techniques in which high data rates can be achieved by the simultaneous transmission over many orthogonal subcarriers [Wan00]. Using MC communications, a wide-band frequency-selective fading channel is divided into many narrow-band frequency non-selective flat fading sub-channels, facilitating channel estimation and equalization as well as time synchronization and narrow band interference mitigation. In addition, the division of the whole bandwidth into many sub-channels provides scalability and flexibility when configuring the communication link.

The most widely used multicarrier modulation technique is OFDM with CP [Li06]. Due to the various advantages of OFDM, it has become the key physical layer transmission technology adopted in current broadband communication systems such as wireless local area networks (WLAN), worldwide interoperability for microwave access (WiMAX), long term evolution (LTE) as well as in digital video and audio broadcasting (DVB, DAB) [Li06] [Kev09]. The OFDM system offers simple implementation using the inverse fast Fourier transforms (IFFT) and the fast Fourier transform (FFT) pairs in the modulator and demodulator parts of the communication system, respectively. However, the large side-lobes of the frequency response of the filters that characterize the subcarrier channels result

in significant interference among subcarriers. In addition, OFDM requires CP and guard band bits result in reducing bandwidth efficiency.

As an alternative to OFDM, FBMC modulation, which is also implemented based on IFFT/FFT pairs, has several advantages over OFDM [Beh11] [Zha10]. Firstly, it does not require CP resulting in better use of the allocated spectrum. Secondly, instead of using a rectangular window, a prototype filter designed with the Nyquist pulse shaping principle is adopted, which can greatly reduce the spectral leakage problem of OFDM. This results in negligible ISI and ICI. Thirdly, the combination of filter banks with offset quadrature amplitude modulation (FBMC/OQAM), known also as OFDM/OQAM, leads to a maximum data transmission rate [Sio02].

Fading channel estimation and equalization techniques are crucial for coherent symbol detection at the receiver. In the framework of multicarrier systems, many channel estimation techniques were proposed in the literature particularly for OFDM systems [Ozd07] [Col02] [Man01] [Che04] [Jam07]. They can be classified as training sequence/pilot symbols based techniques and blind methods. In this thesis, as blind techniques require a large amount of data and have higher complexity than training/pilot based techniques, we will focus our attention on the latter techniques.

Compared to OFDM, few FBMC/OQAM studies have addressed the problem of channel estimation and equalization [Lél08] [Kof13] [Kof11] [Sti10] [Lél12] [Ikh09] [Wal09]. Indeed, when classical channel estimation methods used for OFDM systems are applied directly to FBMC/OQAM system, an intrinsic inter-symbol-interference is observed. This results in system performance degradation. To reduce this intrinsic interference, several

methods are recently proposed, including both preamble-based [Lél08] [Kof13] [Kof11] and scattered pilots-based [Sti10] [Lél12] channel estimators. In [Ikh09], a two stage MMSE equalizer is proposed to cope more efficiently with ICI. A fractionally spaced adaptive decision feedback equalizer (DFE) based on the LMS algorithm was proposed in [Wal09] where the input of each equalizer comprises only the output of each subcarrier.

When dealing with Kalman filter based channel estimators, several approaches were developed for multicarrier systems such as multicarrier code division multiple access (MC-CDMA) and OFDM [Che04] [Jam07] [Kal03]. Indeed, the Kalman filter combined with an autoregressive model to describe the time evolution of the fading channel is shown to track channel variations and to provide superior bit error rate (BER) performance over the standard LMS and RLS estimators [Kal03]. Nevertheless, the AR parameters are unknown and should be estimated. To jointly estimate the autoregressive process and its parameters from noisy observations, the so-called dual Kalman filters based structure [Jam07] [Jam11] can be used. This structure consists of two cross coupled Kalman filters where the first filter uses the latest estimated AR parameters to estimate the fading process, while the second filter uses the estimated fading process to update the AR parameters. In this thesis, we propose to investigate the relevance of the dual Kalman filters for the estimation of FBMC/OQAM time-varying fading channels based on pilot symbols [Ald13]. Once the fading channel coefficients at pilot symbol positions are estimated by the proposed method, the fading channel coefficients at data symbol positions are then estimated by using some interpolation methods such as linear, spline, or low pass interpolation.

The rest of the thesis is organized as follows. In chapter two, we explain the FBMC/OQAM wireless system model where the transmitter, channel and receiver models

are described clearly. In chapter three, we present the estimation of the FBMC/OQAM fading channels based on dual Kalman filters. In chapter four, a comparative simulation study is carried out between the LMS, RLS and dual Kalman filters based channel estimators. Finally, conclusions and future work are drawn in chapter 5.

Chapter 2

FBMC/OQAM Wireless System Model

2.1 Overview

There are different filter bank multicarrier structures that are proposed in the literature. Among them are discrete wavelet multitone (DWMT) [San95], filtered multitone (FMT) [Che00], cosine modulated multitone (CMT) [Lin06], modified discrete Fourier transform (MDFT) [Mir03], exponentially modulated filter bank (EMFB) [Alh03], and FBMC/OQAM [Sio02].

The DWMT is based on the application of M-band wavelet filters that overlap in time, and are designed in order to achieve a sub-channels spectral containment and efficient bandwidth. In addition, DWMT is robust to noise environments and channel variations. Nevertheless, DWMT has high equalizer complexity. To avoid this drawback, FMT can be used. FMT is developed specifically for digital subscriber lines (DSL) application where subcarriers are arranged such that adjacent sub-bands do not overlap. While this makes FMT robust to channel variation, it leads to considerable losses in bandwidth efficiency. To improve bandwidth efficiency, CMT is usually used. In each subcarrier of CMT, a pulse amplitude modulated (PAM) real-valued symbol is transmitted. However, the transmission of real-valued symbols leads to inefficient practical implementation.

Therefore, complex modulated filters such as MDFT, EMFB and FBMC/OQAM are usually used for practical implementations. The MDFT uses complex modulated filter banks that are implemented efficiently using the discrete Fourier transform (DFT). The EMFB uses complex-lapped transform extended to cosine/sine modulated filter banks.

FBMC/OQAM is the most popular filter bank scheme that introduces a half symbol space delay between the in phase and quadrature components of quadrature amplitude modulated (QAM) symbols. This filter bank scheme achieves maximum transmission rate. In addition, FBMC/OQAM uses a specific prototype filter that will reduce the ISI and the ICI. Moreover, the transmitter and receiver in this type could be implemented efficiently in a polyphase structure.

In section 2.2, we describe the FBMC/OQAM structure. In addition, the design of prototype filter based on a frequency sampling technique is introduced. Moreover, we display how the FBMC/OQAM wireless system model is implemented by using polyphase structure to reduce the computational complexity of the FBMC/OQAM wireless system. Transmitter, channel and receiver models of FBMC/OQAM wireless system are presented in sections 2.3, 2.4 and 2.5 respectively. In section 2.6, a comparison between FBMC and OFDM systems will be carried out.

2.2 FBMC/OQAM structure

The general structure of FBMC/OQAM wireless system is shown in the Figure 2.1 which consists of several main processing blocks. At the transmitter side, it consists of OQAM

pre-processing and synthesis filter bank (SFB). At the receiver side, it consists of analysis filter bank (AFB), channel estimation and equalization block[1] and OQAM post-processing.

(a) Transmitter side.

(b) Receiver side.
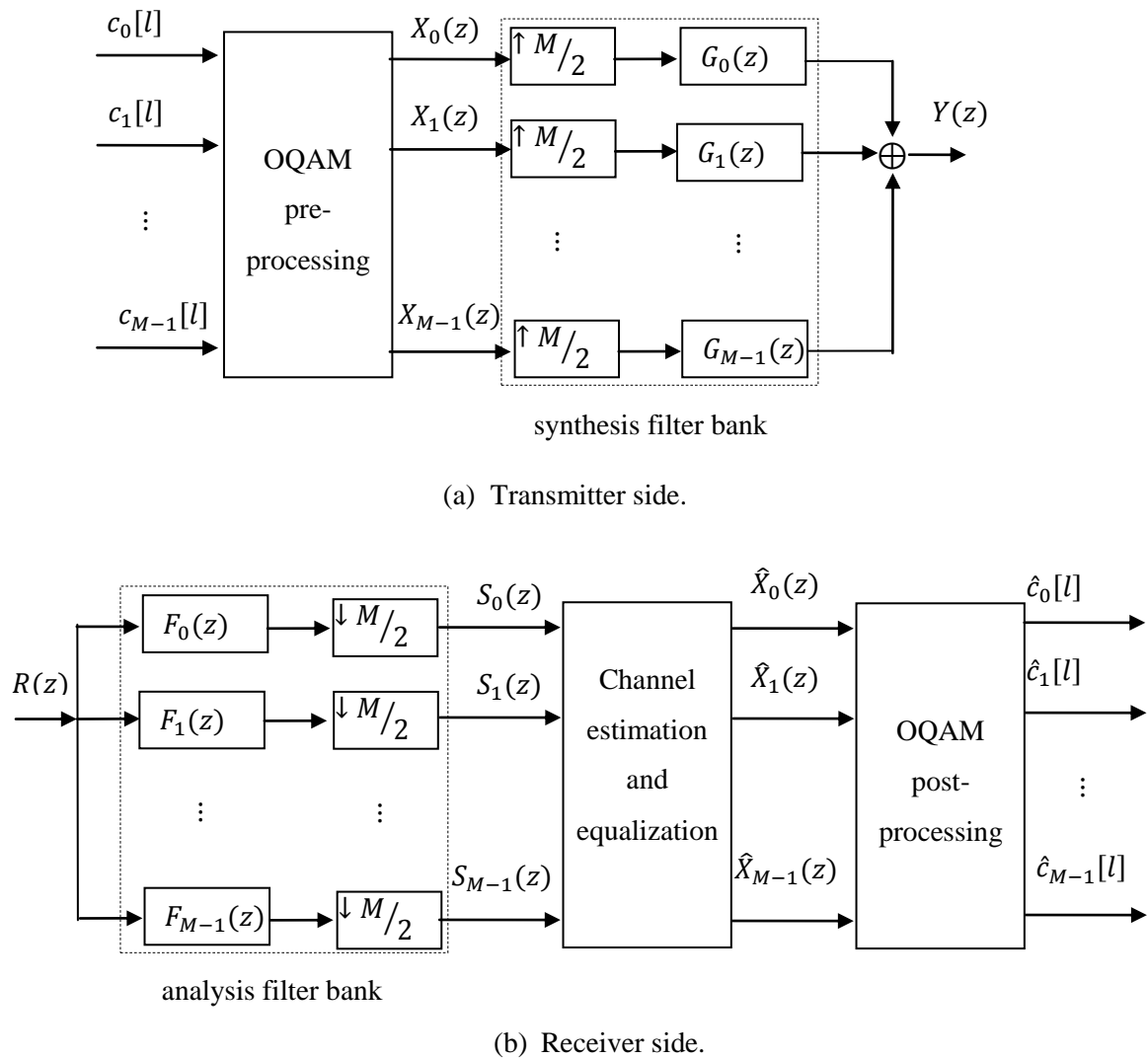
Figure 2.1: General block diagram of FBMC/OQAM wireless system.

2.2.1 OQAM pre/post-processing blocks

In this block, OQAM symbols are transmitted rather than QAM symbols. To perform this modulation, pre/post-processing blocks are placed at the transmitter/receiver sides, respectively.

---

[1] The channel estimation and equalization block will be discussed later in chapter 3.

The block diagram of the OQAM pre-processing is shown in the Figure 2.2 which has two operations. The first operation is complex-to-real conversion, where the real and the imaginary parts of a QAM complex valued symbol $c_k[l]$, transmitted at a rate of $1/T$
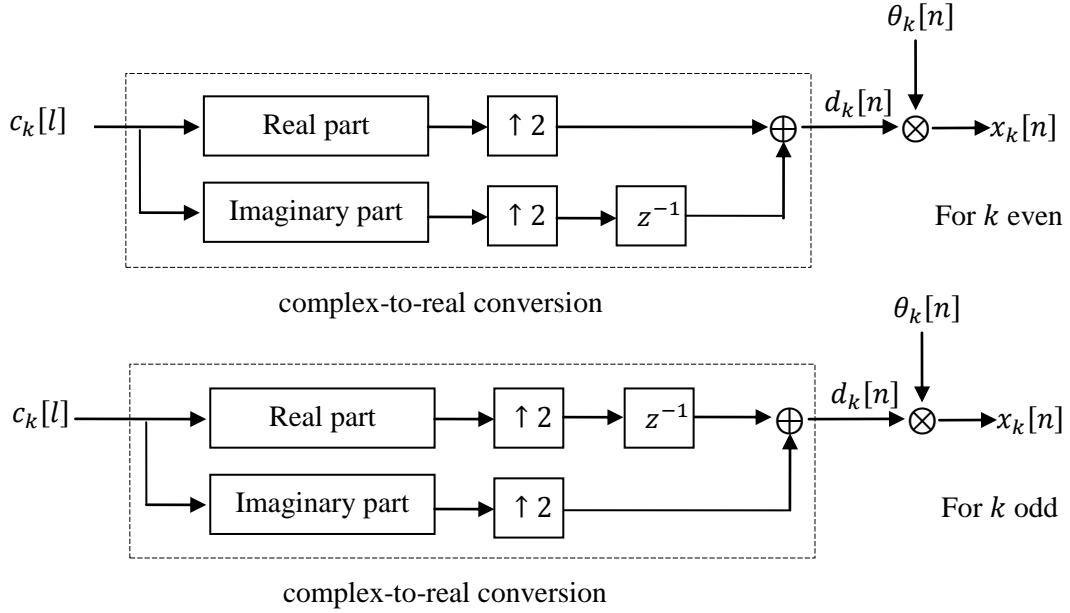
Figure 2.2: Block diagram of OQAM pre-processing.

where the signalling period is defined as $T = 1/\Delta f$ with Δf is the subcarrier spacing, are separated to form two new symbols $d_k[n]$ and $d_k[n+1]$. The complex-to-real conversion is different for even and odd numbered sub-channels and are given by the following equations:

$$d_k[n] = \begin{cases} Re(c_k[l]), & k \ even \\ Im(c_k[l]), & k \ odd \end{cases} \tag{2.1}$$

$$d_k[n+1] = \begin{cases} Im(c_k[l]), & k \ even \\ Re(c_k[l]), & k \ odd \end{cases} \tag{2.2}$$

where l is the sample index at *OQAM pre-processing input / post-processing output* and n is the sample index at *OQAM pre-processing output / post-processing input*. Note that complex-to-real conversion increases the sample rate by factor 2. The second operation of

the OQAM pre-processing block is the multiplication by $\theta_k[n]$ in order to maintain orthogonal symbols.

$$\theta_k[n] = j^{k+n} \tag{2.3}$$

Then, the output data of the pre-processing block $x_k[n]$ can be expressed as:

$$x_k[n] = d_k[n]\theta_k[n] \tag{2.4}$$

The block diagram of the OQAM post-processing is shown in Figure 2.3. It consists of two main operations. The first one is the multiplication by the complex conjugate of $\theta_k[n]$, denoted by $\theta^*_k[n]$, followed by taking the real part. The second operation is real-to-complex conversion, in which two successive real valued symbols form a complex valued symbol denoted by $\hat{c}_k[l]$ and defiend as follows:

$$\hat{c}_k[l] = \begin{cases} \hat{d}_k[n] + j\hat{d}_k[n+1], & k \ even \\ \hat{d}_k[n+1] + j\hat{d}_k[n], & k \ odd \end{cases} \tag{2.5}$$

In this sense the real-to-complex conversion decreases the sample rate by factor 2.
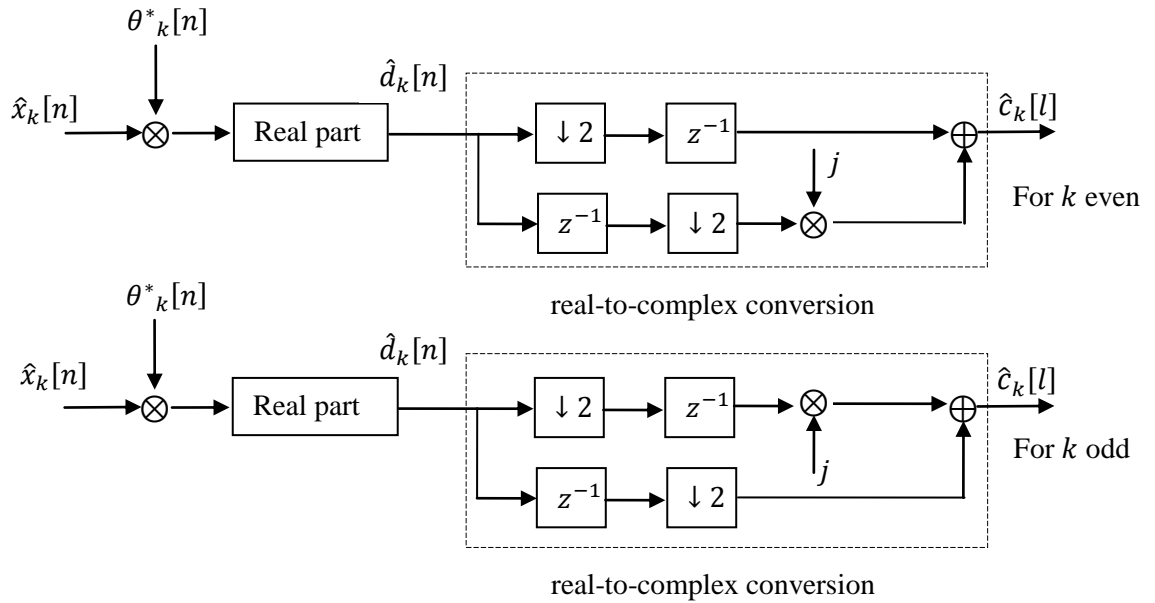
Figure 2.3: Block diagram of OQAM post-processing.

9

2.2.2 Synthesis and analysis filter bank blocks

At the transmitter, M upsamplers and M synthesis filters will form synthesis filter bank. The data $X_k(z)$ is then up sampled by $M/2$ and filtered with synthesis filters $G_k(z)$. Finally all sub-channels are added together to form $Y(z)$. At the receiver, M down samplers and M analysis filters will form analysis filter bank such that the signal $R(z)$ is filtered with analysis filters $F_k(z)$, and then down sampled by $M/2$ to form $\hat{X}_k(z)$.

In order to achieve high spectral efficiency, complex modulated filter banks [Vai93] are usually used. This means that all sub-channel filters are frequency shifted versions of a single real-valued linear-phase finite impulse response (FIR) low-pass prototype filter $p[m]$ by using exponential modulation [Bel09]. Thus, the kth synthesis filter $g_k[m]$ can be expressed as:

$$g_k[m] = p[m]exp\left(j\frac{2\pi k}{M}\left(m - \frac{L_p - 1}{2}\right)\right) \qquad (2.6)$$

where $m = 0,1,...,L_p - 1$, M is the number of sub-channels typically a power of two, and L_p denotes to the prototype filter length which is chosen to be $L_p = KM - 1$, where K is overlapping factor[2].

In addition, the kth analysis filter $f_k[m]$ is simply a time-reversed and complex-conjugated version of the corresponding synthesis filter [Vai93]:

---

[2] Overlapping factor is defined as the number of multicarrier symbols which overlap in the time domain. Usually, K is an integer number.

$$f_k[m] = g_k^*[L_p - 1 - m]$$

$$= p^*[L_p - 1 - m]exp^*\left(j\frac{2\pi k}{M}\left(L_p - 1 - m - \frac{L_p - 1}{2}\right)\right)$$

$$= p[L_p - 1 - m]exp^*\left(j\frac{2\pi k}{M}\left(-m + \frac{L_p - 1}{2}\right)\right)$$

$$= p[L_p - 1 - m]exp^*\left(-j\frac{2\pi k}{M}\left(m - \frac{L_p - 1}{2}\right)\right)$$

$$= p[L_p - 1 - m]exp\left(j\frac{2\pi k}{M}\left(m - \frac{L_p - 1}{2}\right)\right)$$

$$(2.7)$$

2.2.2.1 Design of prototype filter

In order to avoid ISI problem the channel must satisfy the Nyquist criterion when having ideal case. Now, if the symbol period is T_s and the symbol rate is $f_s = 1/T_s$, the channel frequency response must be symmetrical about the frequency $f_s/2$. Accordingly, in FBMC, the prototype filter for the synthesis and analysis filter banks must be half-Nyquist, which means that the square of its frequency response must satisfy the Nyquist criterion.

The design of the prototype filter must satisfy perfect reconstruction (PR) conditions or at least provide nearly perfect reconstruction (NPR) characteristics. However, the PR property is only achieved under the condition of ideal transmission channel. As interferences in the wireless channel are unavoidable, there is no way to have PR conditions. Thus, prototype filters are designed to satisfy NPR characteristics [Bel01].

There are different methods to design NPR prototype filter such as frequency sampling technique [Bel01], or windowing based techniques [Mar08]. In these methods, prototype filter coefficients can be given using a closed-form representation that includes only a few

adjustable design parameters. In this thesis, we focus our attention on frequency sampling technique.

The impulse response coefficients of the filter are obtained according to the desired frequency response, which is sampled on a KM uniformly spaced frequency points $\omega_k = \frac{2\pi k}{KM}$. Thus, the FIR low-pass prototype filter $p[m]$ can be written as [Vih09]:

$$p[m] = \frac{1}{KM} \left(\hat{P}[0] + 2 \sum_{k=1}^{U} (-1)^k \hat{P}[k] \cos\left(\frac{2\pi k}{KM} (m+1) \right) \right) \qquad (2.8)$$

where $m = 0,1,\dots,L_p - 1$, and

$$\begin{cases} \hat{P}[0] = 1 \\ \hat{P}[k]^2 + \hat{P}[K-k]^2 = 1, \quad for\ k = 1,2,\dots,\dfrac{K}{2} \\ \hat{P}[k] = 0, \quad for\ k = K, K+1, \dots, U = \dfrac{KM-2}{2} \end{cases} \qquad (2.9)$$

The frequency response and the impulse response for the prototype filter used in FBMC/OQAM wireless system with different values of overlapping factor are shown respectively in Figure 2.4 and Figure 2.5 with $M = 16$ and $L_p = KM - 1$.
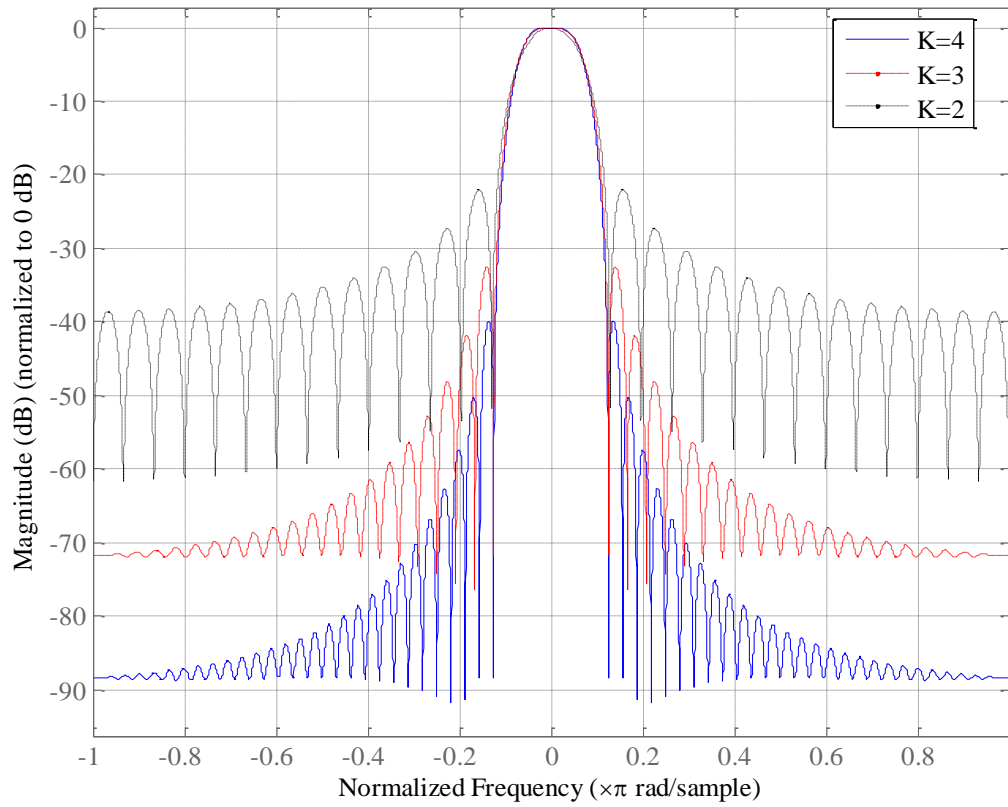
Figure 2.4: Frequency response of prototype filter with $M = 16$ and $L_p = KM - 1$.
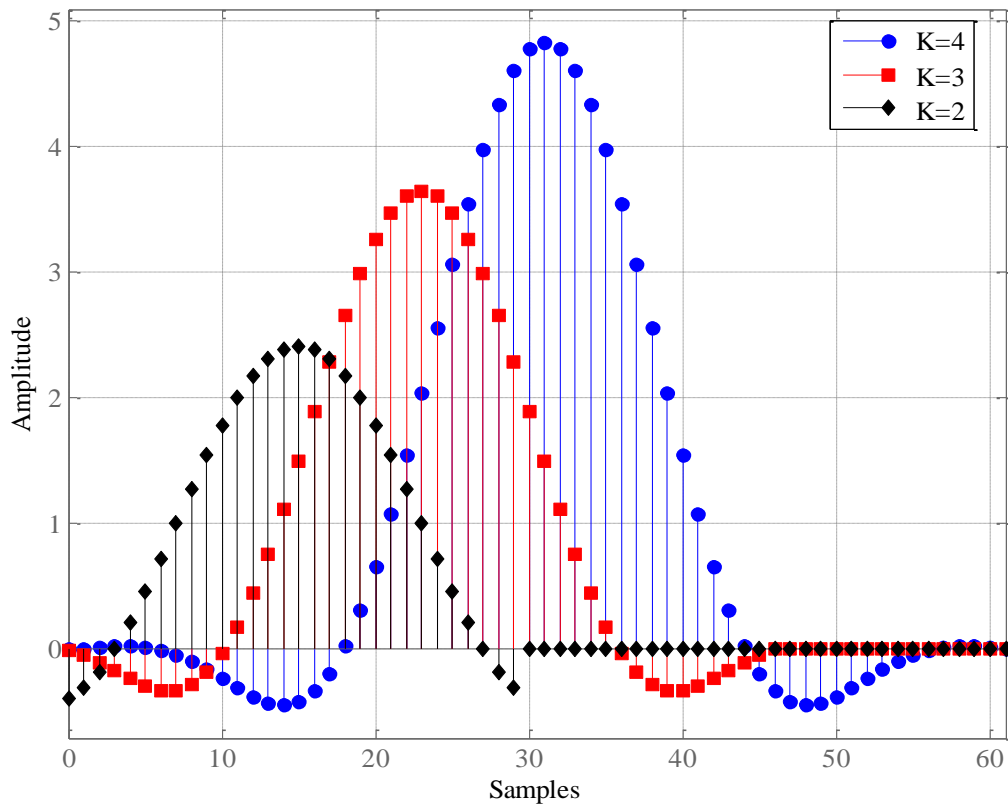
Figure 2.5: Impulse response of prototype filter with $M = 16$ and $L_p = KM - 1$.

2.2.2.2 Polyphase structure

The synthesis filter bank (SFB) and the analysis filter bank (AFB) of FBMC/OQAM wireless system introduce high computational complexity because they are performed at the high sampling rate leading to a huge amount of unnecessary calculations. Nevertheless, the computational complexity can be reduced by exploiting polyphase representations of SFB and AFB with IFFT/FFT operations. The polyphase can offer drastic simplifications because filtering operations are done at the lower sampling rate and avoiding unnecessary calculations.

In the case of modulated filter banks, the number of polyphase filter branches depends on the periodicity of the modulation function, denoted by $\xi_k[m]$, and can be written as follows:

$$
\begin{aligned}
\xi_k[m] \quad &= \exp\left(j\frac{2\pi k}{M}\left(m - \frac{L_p - 1}{2}\right)\right) \\
&= \exp\left(-j\frac{2\pi k}{M}\left(\frac{L_p-1}{2}\right)\right)\exp\left(j\frac{2\pi km}{M}\right) \\
&= \beta_k\gamma_k[m]
\end{aligned}
\tag{2.10}
$$

Here, we can express $\gamma_k[m]$ and β_k separately as follows:

$$
\gamma_k[m] = \exp\left(j\frac{2\pi km}{M}\right)
\tag{2.11}
$$

$$
\beta_k[n] = (-1)^{kn}\exp\left(-j\frac{2\pi k}{M}\left(\frac{L_p - 1}{2}\right)\right)
\tag{2.12}
$$

Note that we add a simple extra term $(-1)^{kn}$ to β_k to make it is possible to frequency shift all sub-channel signals around zero frequency [Sti10].

Now, suppose:

$$m = q + tM \tag{2.13}$$

where $q = 0,1, \dots, M - 1$ and $t = 0,1, \dots, K - 1$

Because $\gamma_k[m] = \gamma_k[q + tM]$, then the kth synthesis filter $G_k(z)$ can be expressed in the form of polyphase filters as follows:

$$
\begin{aligned}
G_k(z) &= \sum_{m=0}^{L_p-1} p[m]\xi_k[m]z^{-m} \\
&= \sum_{q=0}^{M-1}\sum_{t=0}^{K-1} p[q + tM]\beta_k\gamma_k[q + tM]z^{-(q+tM)} \\
&= \sum_{q=0}^{M-1} \beta_k\gamma_k[q + tM]z^{-q} \sum_{t=0}^{K-1} p[q + tM]z^{-tM} \\
&= \beta_k \sum_{q=0}^{M-1} \gamma_k[q]z^{-q}A_q(z^M)
\end{aligned}
\tag{2.14}
$$

We can write this form in matrix notation as:

$$\boldsymbol{G}(z) = \boldsymbol{\beta}.\boldsymbol{W}.\boldsymbol{A}(z).\boldsymbol{O}(z) \tag{2.15}$$

where:

$\boldsymbol{G}(z) = [G_0(z)G_1(z) \cdots G_{M-1}(z)]^T$

$\boldsymbol{\beta} = diag[\, \beta_0\, \beta_1 \cdots \beta_{M-1}]$

$\boldsymbol{W} = M\gamma_k(q)$

$\boldsymbol{A}(z) = diag[A_0(z)A_1(z) \cdots A_{M-1}(z)]$

$\boldsymbol{O}(z) = \begin{bmatrix} 1 & z^{-1} \cdots & z^{-(M-1)} \end{bmatrix}^T$

Equation (2.15) shows that the synthesis filter bank consists of $\beta_k[n]$ multipliers, IFFT, synthesis polyphase filtering $A_q(z)$, upsamplers by $M/2$ and delay chain.

So, we can redraw the SFB block of the FBMC/OQAM wireless system as shown in the Figure 2.6:
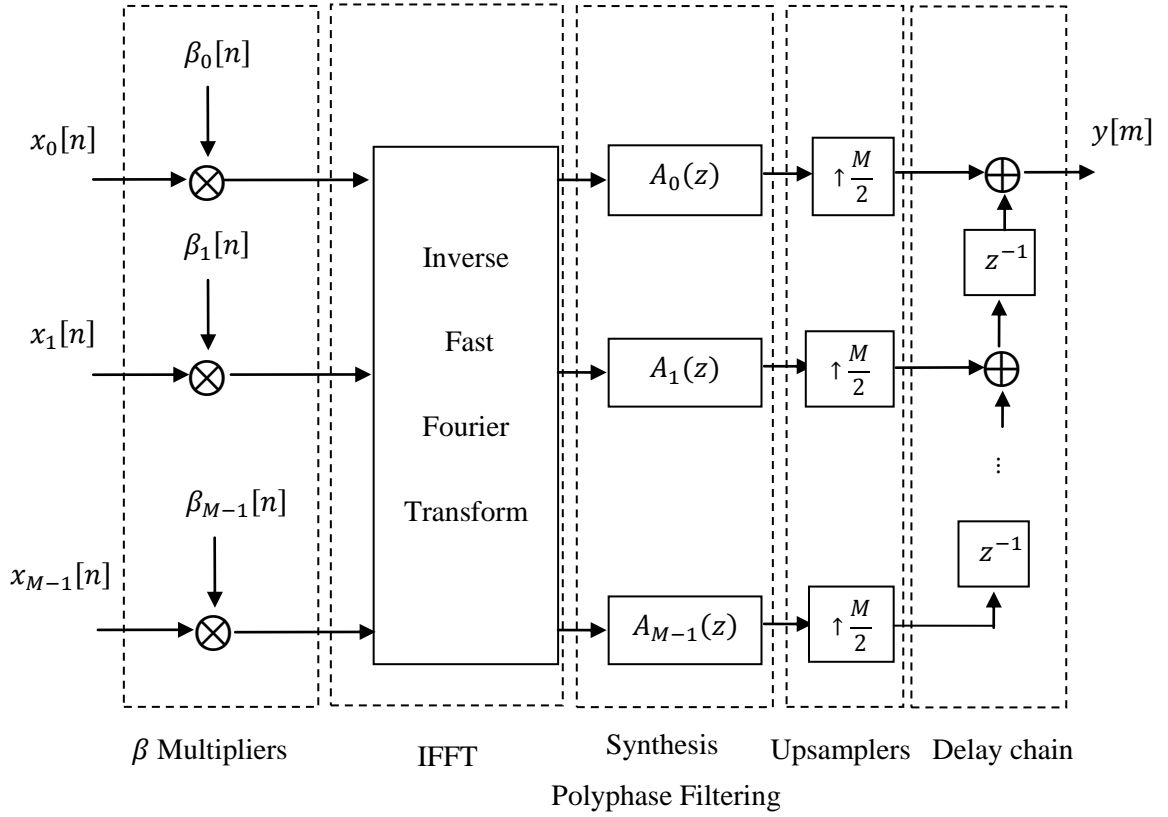
Figure 2.6 Block diagram of SFB using polyphase structure.

Next, we can write the polyphase decomposition of the kth analysis filter $F_k(z)$ as follows:

$$F_k(z) = \sum_{m=0}^{L_p-1} p[L_p - 1 - m]\xi^*_k[m]z^{-m}$$

$$= \beta^*_k \sum_{q=0}^{M-1} \gamma^*_k[q]z^{-(M-1-q)}B_q(z)$$

(2.16)

where $B_q(z) = A_{M-1-q}(z)$.

Note that we can write equation (2.17) in matrix notation as follows:

$$\boldsymbol{F}(z) = \boldsymbol{\beta}^*.\boldsymbol{W}^*.\boldsymbol{B}(z)N(z)$$

(2.17)

where:

$$\boldsymbol{F}(z) = [\,F_0(z)F_1(z)\cdots F_{M-1}(z)]^T$$

$$\boldsymbol{B}(z) = diag[B_0(z)B_1(z)\cdots B_{M-1}(z)]$$

$$\boldsymbol{N}(z) = \begin{bmatrix} z^{-(M-1)} & z^{-(M-2)} & \cdots & z^{-1} & 1 \end{bmatrix}^T$$

Equation (2.18) shows that the analysis filter bank consists of delay chain, downsamplers by $M/2$, analysis polyphase filtering $B_q(z)$, FFT, and $\beta_k^*[n]$ multipliers. Thus, we can redraw the AFB of the FBMC/OQAM wireless system as shown in Figure 2.7.
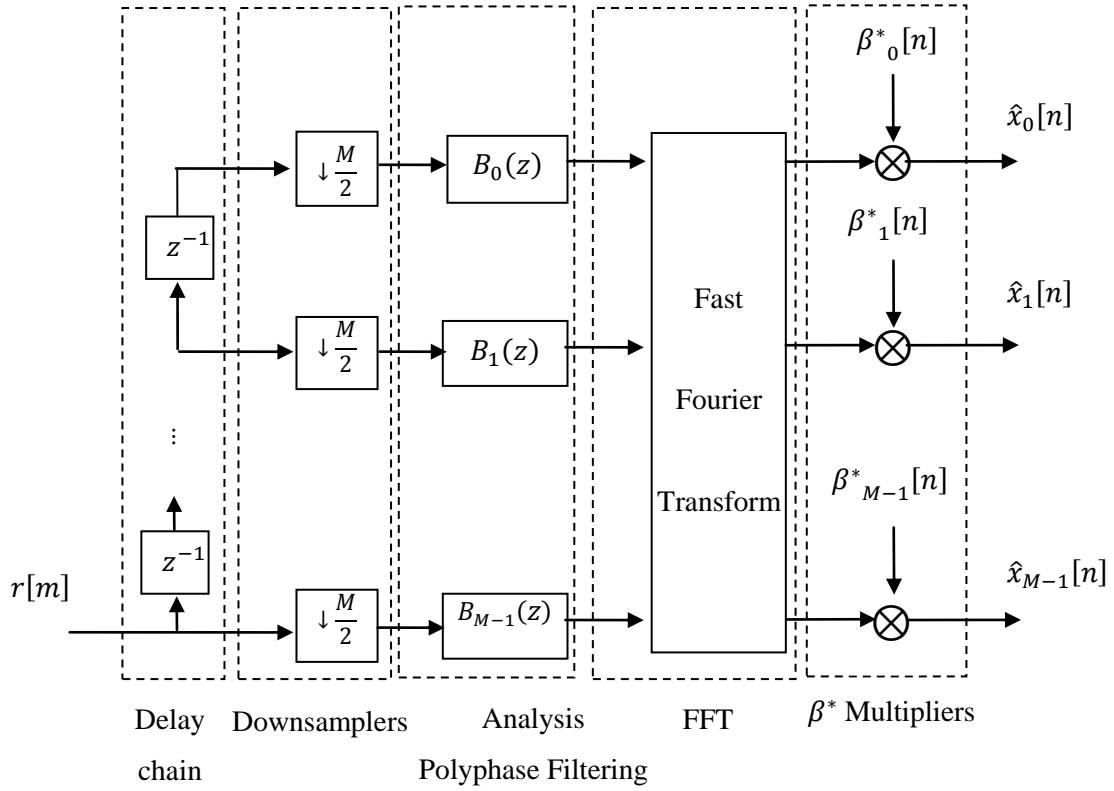
Figure 2.7: Block diagram of AFB filters using polyphase structure.

The analysis polyphase filter at the receiver in time index can be expressed as follows:

$$b_k(m) = a_{M-1-k}(m) = p(M-1-k+mM) \tag{2.18}$$

2.2.2.3 Computational complexity issue

The polyphase structure will reduce the computational complexity of the system model compared to the general structure of FBMC/OQAM system without polyphase. When polyphase structure is included in FBMC/OQAM system, then the total number of real multiplications for SFB (O_{SFB}) is the sum of the multiplications in each processing block: pre-processing, β_k multipliers, M point IFFT, and M branch polyphase filter section, i.e.

$$O_{SFB} = 2\big(2M + \big((log_2(M) - 3) + 4\big) + 2KM\big) \qquad (2.19)$$

Here, the pre-processing section is considered to be multiplication free because it only consists of trivial multiplications by ± 1 and $\pm j$. Moreover, the first multiplication by 2 is because a complex-valued QAM symbol is separated into two OQAM symbols. The complexity of AFB is equal to the complexity of SFB because similar processing blocks are used but in the reverse order. Thus, the total complexity of the FBMC/ OQAM system:

$$\qquad (2.20)$$

When polyphase structure is not used in FBMC/OQAM system, the total number of real multiplications for SFB is:

$$O_{SFB} = 2(M.KM) \qquad (2.21)$$

Then, the total complexity of the FBMC/ OQAM system:

$$O_{FBMC/OQAM}^{without\_polyphase} = O_{SFB} + O_{AFB} = 4(M.KM) \qquad (2.22)$$

The number of real multiplications as a function of number of sub-channels in the case of FBMC with different overlapping factor is shown in the Figure 2.8:
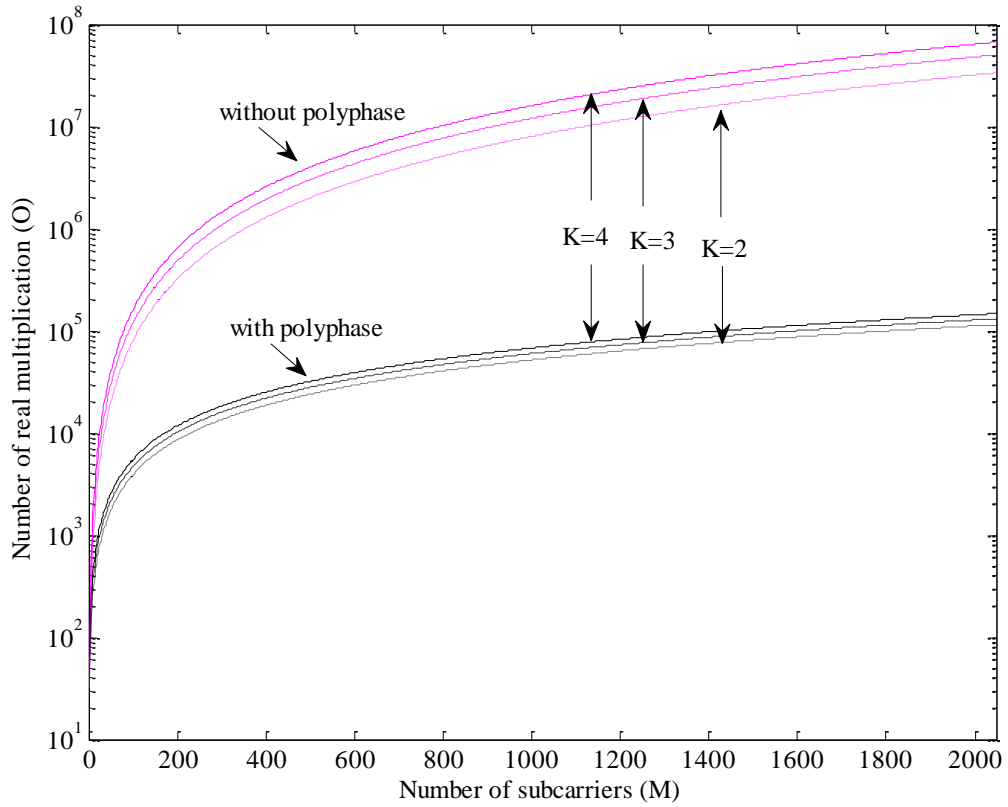
Figure 2.8: The number of real multiplications as a function of number of sub-channels for FBMC.

2.3 Transmitter model

The Block diagram of the FBMC/OQAM transmitter is shown in the Figure 2.9.
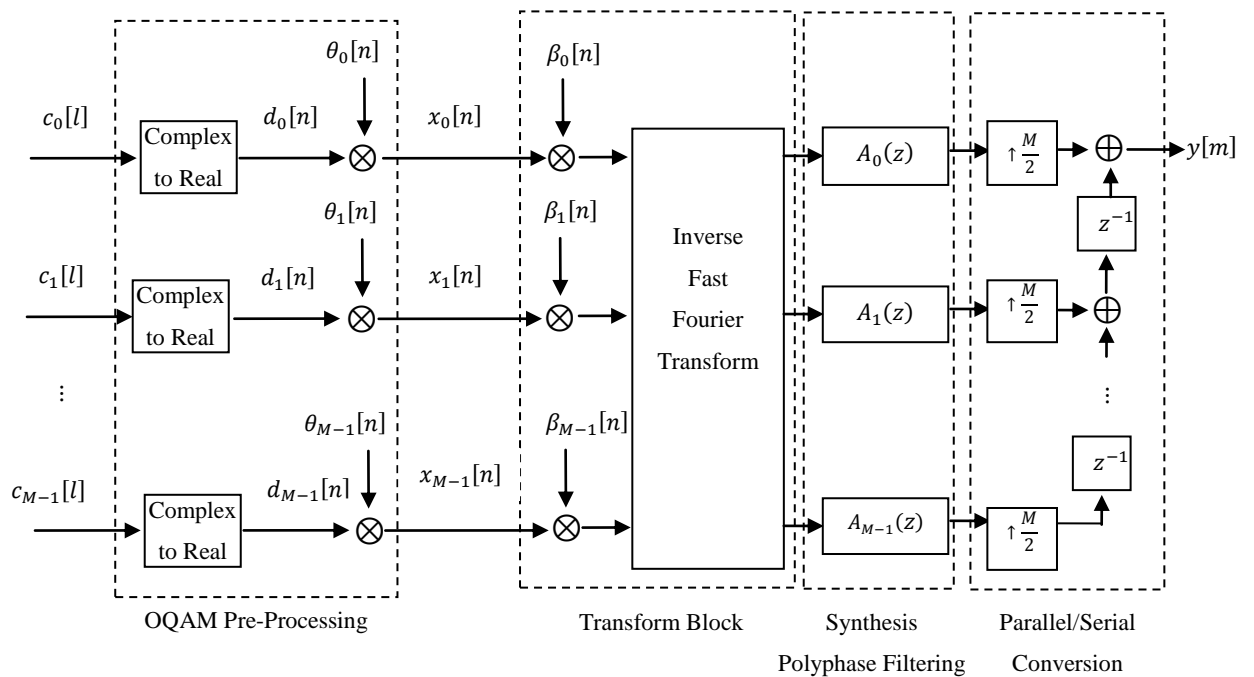
Figure 2.9: Block diagram of the FBMC/OQAM transmitter.

The transmitted signal can be written in matrix notation as:

$$Y(z) = G^T(z).X(z^{M/2})$$

$$= (\beta.W.A(z).O(z))^T.X(z^{M/2}) \qquad (2.23)$$

$$= O^T(z).A(z).W.\beta.X(z^{M/2})$$

where $X(z^{M/2}) = [X_0(z^{M/2})X_1(z^{M/2}) \cdots X_{M-1}(z^{M/2})]^T$

Also, the discrete-time baseband signal at the output of the synthesis filter bank of the FBMC transmitter based on OQAM modulation can be expressed as [Bel09]:

$$y[m] = \sum_{k=0}^{M-1} \sum_{n=-\infty}^{\infty} x_k[n]\beta_k[n]p\left[m - n\frac{m}{2}\right]e^{j\frac{2\pi}{M}km}$$

$$\qquad (2.24)$$

$$= \sum_{k=0}^{M-1} \sum_{n=-\infty}^{\infty} d_k[n]\theta_k[n]\beta_k[n]p\left[m - n\frac{m}{2}\right]e^{j\frac{2\pi}{M}km}$$

where m is the sample index at *SFB output / AFB input*, and M is the number of subcarriers in the filter bank.

2.4 Channel model

The simplest channel is the free space line of sight (LOS) channel with no objects between the receiver and the transmitter or around the path between them. In this simple case, the transmitted signal attenuates since the energy is spread spherically around the transmitting antenna. Another case is none line of sight (NLOS). In this case the path between the base station and mobile stations of mobile communications is characterized by reflection, diffraction, and scattering of radio waves from objects such as buildings, hills, trees, etc. As a result, the received signal consists of a superposition of several delayed and

attenuated copies of the transmitted signal. This gives rise to frequency-selective fading which spreads the transmitted signal in time and, hence, leads to ISI. When all multi-paths arrive at the receiver within the symbol duration, the resulting fading is called frequency non- selective fading or flat fading. In addition to multi-path fading, due to the relative motion between the transmitter and the receiver and the movement of surrounding objects, the received signal is subject to Doppler shifts. This gives rise to time-varying fading. Hence, the transmitted signal through a mobile wireless channel may be generally affected by time-varying frequency-selective fading.

The transmitted FBMC/OQAM signal $y[m]$ in (2.25) is assumed to go through a time-varying frequency-selective Rayleigh fading channel $h_k[m]$ with background additive white Gaussian noise (AWGN) as shown in the Figure 2.10. Assuming that the allocated bandwidth for each subcarrier is less than the coherence bandwidth of the wireless channel, each subcarrier will undergo frequency non-selective flat-fading.
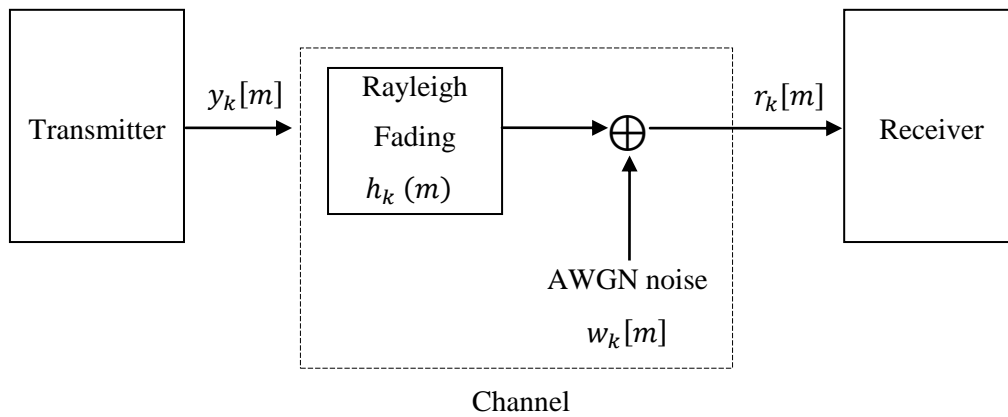
Figure 2.10: Block diagram of channel model

According to Jakes [Jak74], the frequency non-selective flat fading process over the mth FBMC/OQAM symbol can be modeled as a sum of L_s scatterers given as a sum of weighted complex exponentials:

$$h_k[m] = \sum_{l=1}^{L_s} g_{kl}e^{j(2\pi f_d m cos\varphi_{kl}+\vartheta_{kl})} \qquad (2.25)$$

where g_{kl}, φ_{kl} and ϑ_{kl} are, respectively, the random scattered amplitude, angle of arrival and initial phase associated with the lth scatterer, k^{th} carrier and the mth FBMC/OQAM symbol and f_d is Doppler frequency.

When there are a large number of scatterers, $h_k[m]$ can be approximated as a complex Gaussian process $h_k[m] = |h_k[m]|e^{-j\varphi_k[m]}$. In an environment with no direct line-of-sight path between the transmitter and the receiver, the fading process $h_k[m]$ will have zero-mean. In that case, the phase $\varphi_k[m]$ is uniformly distributed on $[0,2\pi]$ and the envelope $|h_k[m]| = \hbar$ has a Rayleigh probability density function defined as follows:

$$f_\hbar[\hbar] = \begin{cases} \dfrac{\hbar}{\sigma_\hbar^2}e^{-\hbar^2/2\sigma_\hbar^2}, & \hbar \geq 0 \\ 0, & otherwise \end{cases} \qquad (2.26)$$

where $\sigma_\hbar^2 = E[|h_k[m]|^2]$ is the variances of the fading processes $\{h_k[m]\}_{k=0,1,...,M-1}$. A typical Rayleigh fading envelope and phase of a time-varying fading process $h_k[m]$ are shown, respectively, in the Figure 2.11 and Figure 2.12 with Doppler rate $f_d T_s = 0.05$.
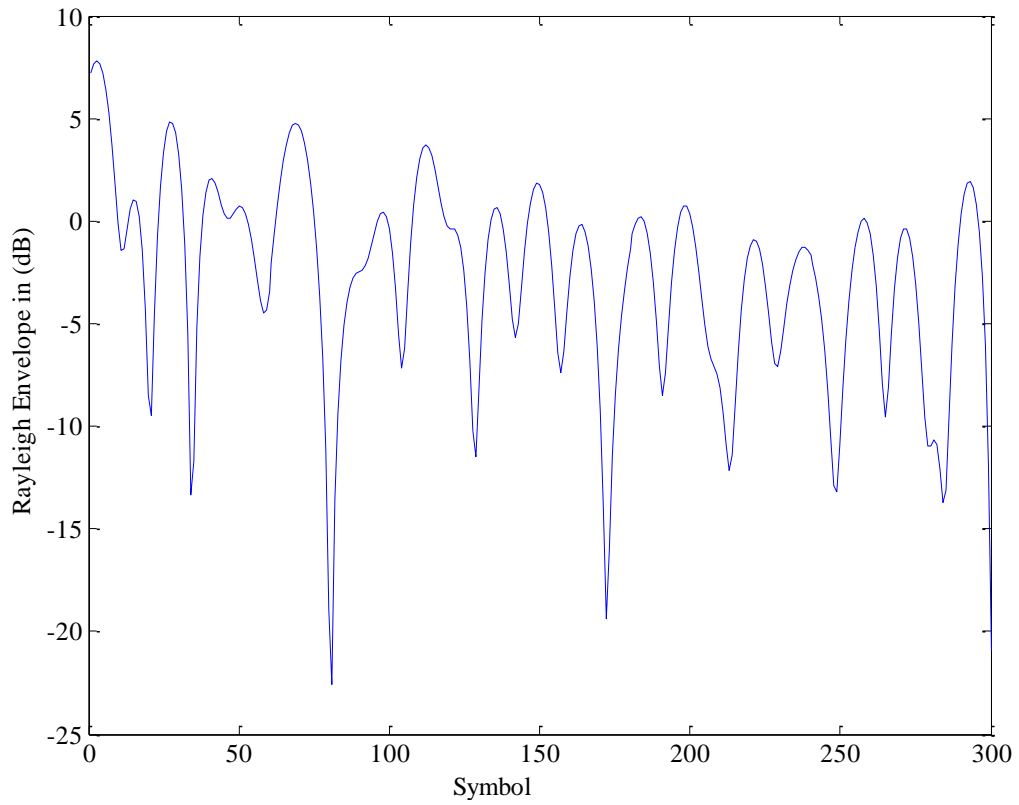
Figure 2.11: Rayleigh envelope of $h_k[m]$ along the mth FBMC/OQAM symbol.
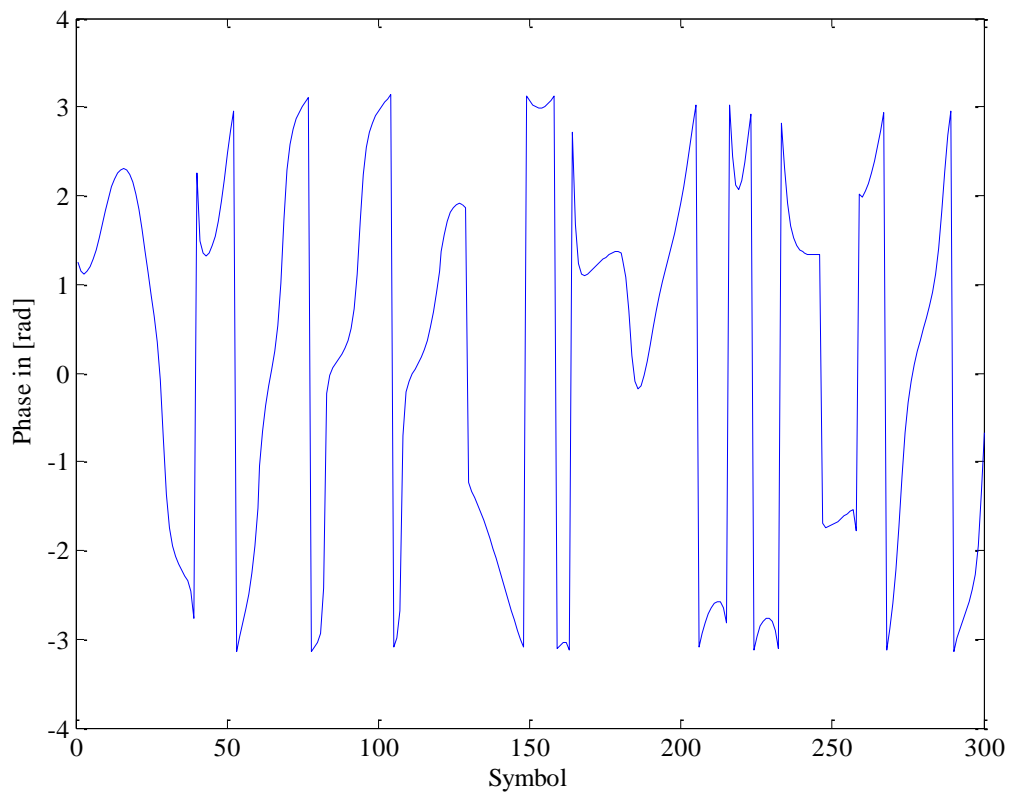
Figure 2.12: Phase of $h_k[m]$ along the mth FBMC/OQAM symbol.

The statistical properties of the fading process $h_k[m]$ are given by its power spectrum density (PSD) and autocorrelation function (ACF) as shown in the Figure 2.13 and Figure 2.14, respectively. Indeed, the PSD of $h_k[m]$ is defined by the well-known U-shaped band-limited Jakes spectrum with maximum Doppler frequency f_d:

$$S(f) = \begin{cases} \dfrac{1}{\pi f_d \sqrt{1 - (f/f_d)^2}}, & |f| \leq f_d \\ 0 & , \quad elsewhere \end{cases} \tag{2.27}$$

where $f_d = {v}/{\lambda}$ with v is the mobile speed and λ is the wave length of the carrier wave. The corresponding normalized discrete-symbols autocorrelation function (ACF) hence satisfies:

$$R_k = J_0(2\pi f_d T_s |k|) \tag{2.28}$$

where $J_0(.)$ is the zero-order Bessel function of the first kind, T_s is the symbol period, and $f_d T_s$ denotes the Doppler rate.
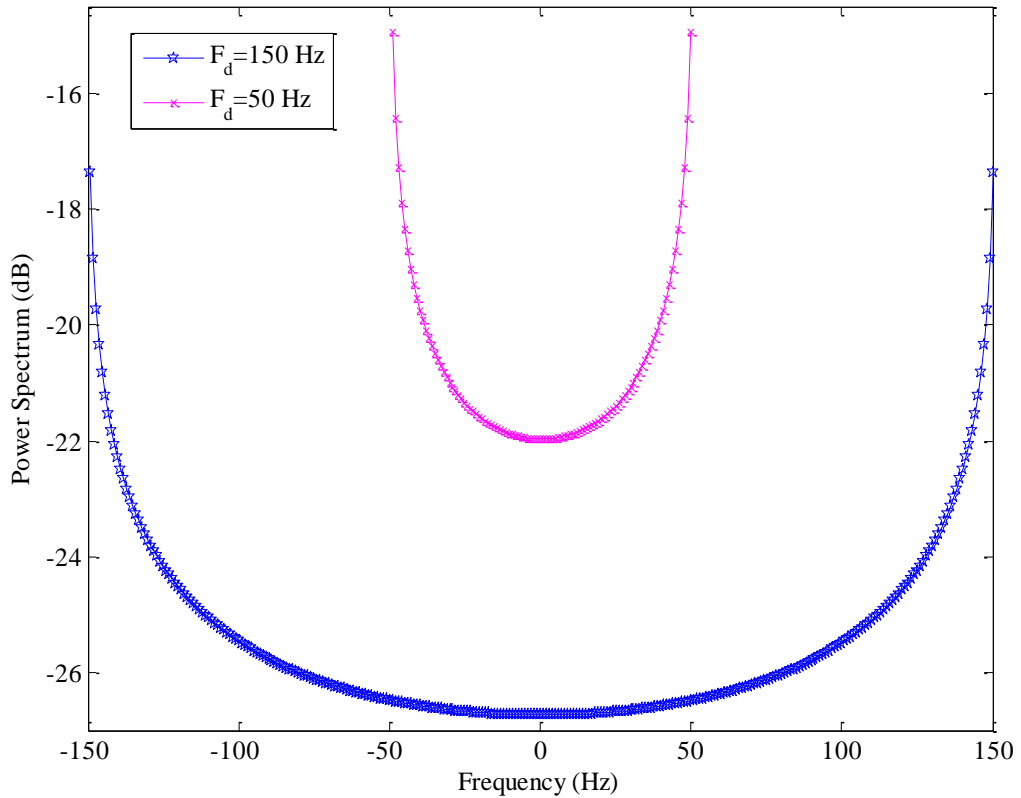
Figure 2.13: Power spectrum density of h_k [m] along m^{th} FBMC/OQAM symbol.
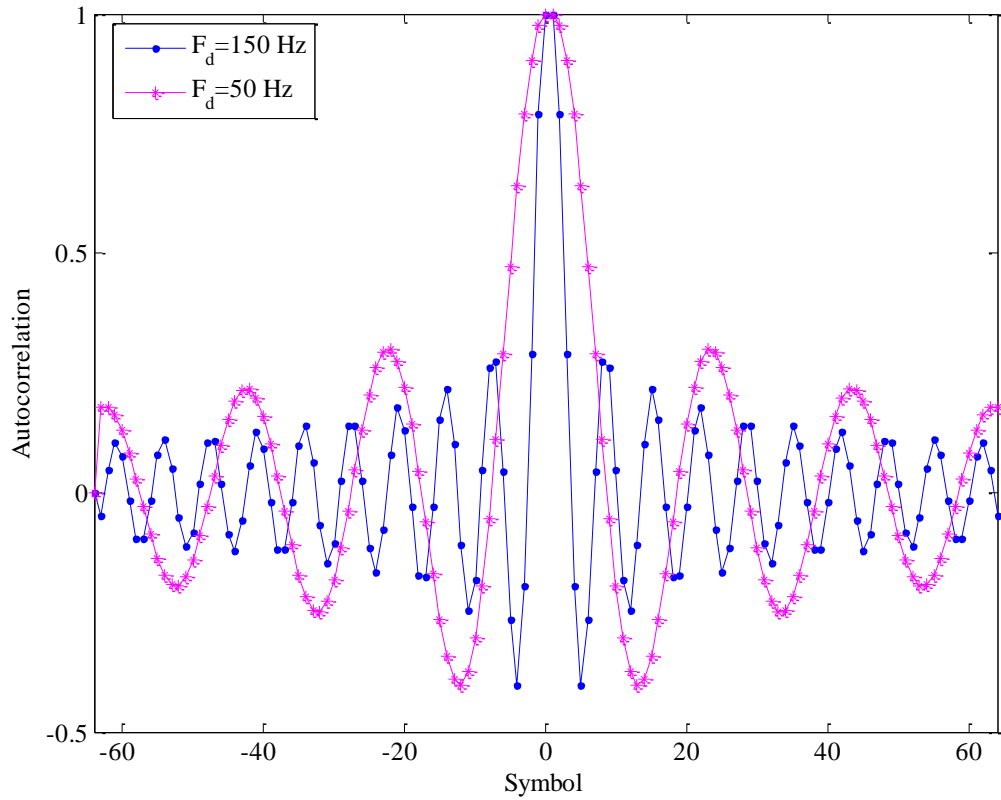
Figure 2.14: Autocorrelation function of h_k *[m]* along m^{th} FBMC/OQAM symbol.

2.5 Receiver model

The block diagram of the FBMC/OQAM receiver is shown in Figure 2.15.
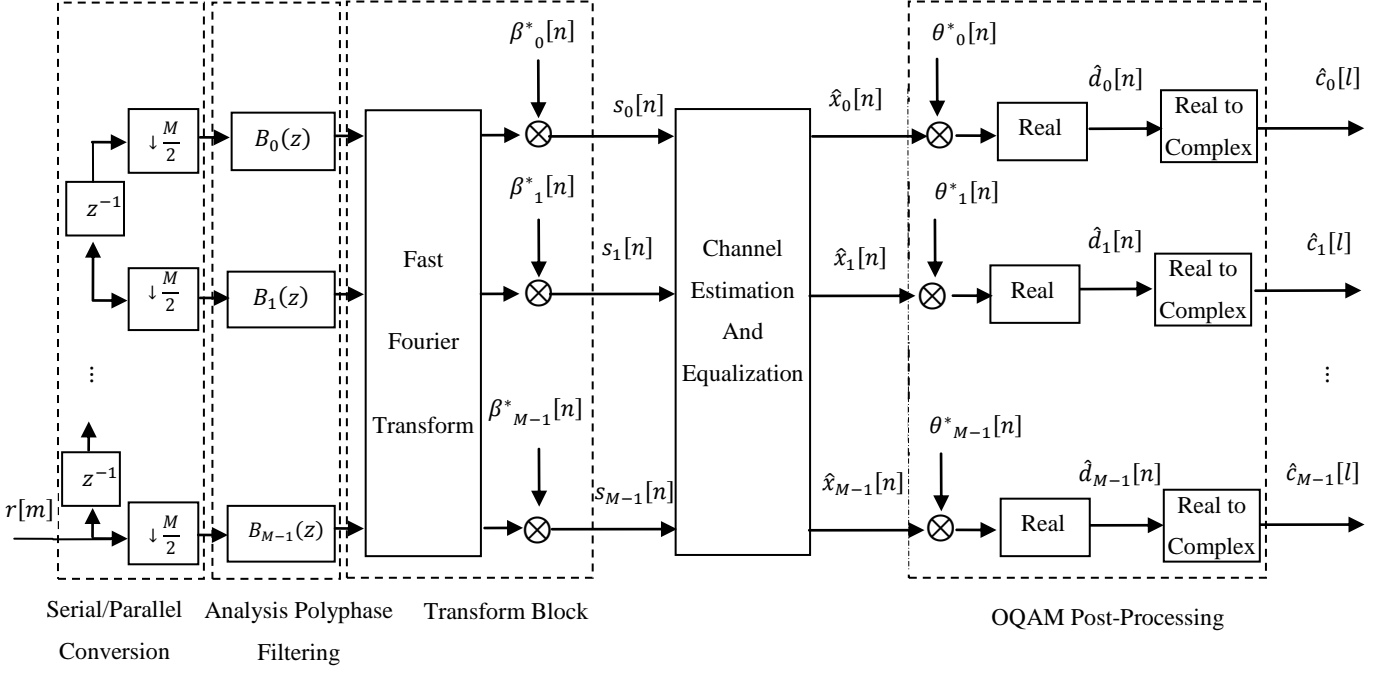
Figure 2.15: Block diagram of the FBMC/OQAM receiver.

After the transmitted signal goes through the wireless channel, the received signal sample over the kth subcarrier for the mth FBMC/OQAM symbol can be expressed as:

$$r_k[m] = y_k[m]h_k[m] + w_k[m] \qquad (2.29)$$

where $h_k[m]$ is a complex valued fading process over the kth subcarrier for the mth FBMC/OQAM symbol, $w_k[m]$ is an additive white Gaussian noise (AWGN) process. The noise processes $\{w_k[m]\}_{k=0,1,\ldots,M-1}$ are assumed to be mutually independent and identically distributed zero-mean complex Gaussian processes, with equal variances σ_w^2.

After processing the received signal $r_k[m]$ with the analysis filter bank block, the resulting signal at the input of channel estimation and equalization is given by:

$$s_k[n] = \left[r_k[m] * f_k[m]\right]_{\downarrow\frac{M}{2}} = x_k[n].q_k[n] + \eta_k[n] \qquad (2.30)$$

26

where $q_k[n] = \left[h_k[m]g_k[m] * f_k[m]\right]_{\downarrow \frac{M}{2}}$ with $*$ denotes the convolution operator, and

$\eta_k[n]$ is a Gaussian noise process with variance σ_η^2. Under the assumption of nearly perfect

reconstruction (NPR) conditions of the prototype filter, it follows that the value of

$g_k[m] * f_k[m]$ is small valued contribution, and will be ignored from now [Sti10]. Under

this assumption, it follows that $q_k[n] = \left[h_k[m]g_k[m] * f_k[m]\right]_{\downarrow \frac{M}{2}} \cong h_k[n]$. Thus, equation

(2.30) is reduced to:

$$s_k[n] = x_k[n]h_k[n] + \eta_k[n], \quad k = 0,1,\dots,M-1 \qquad (2.31)$$

2.6 FBMC/OQAM versus OFDM

The main difference between FBMC and OFDM is the choice of the prototype filter. The

OFDM system uses a rectangular window filter whereas the FBMC system uses a

prototype filter designed with the Nyquist pulse shaping principle, which can reduce

greatly the spectral leakage problem of OFDM. This results in negligible ISI and ICI. The

frequency response and the impulse response for the prototype filters that are used in

FBMC and OFDM are shown in the Figure 2.16 and the Figure 2.17 respectively with

$M = 16, K = 4$ and $L_p = 63$
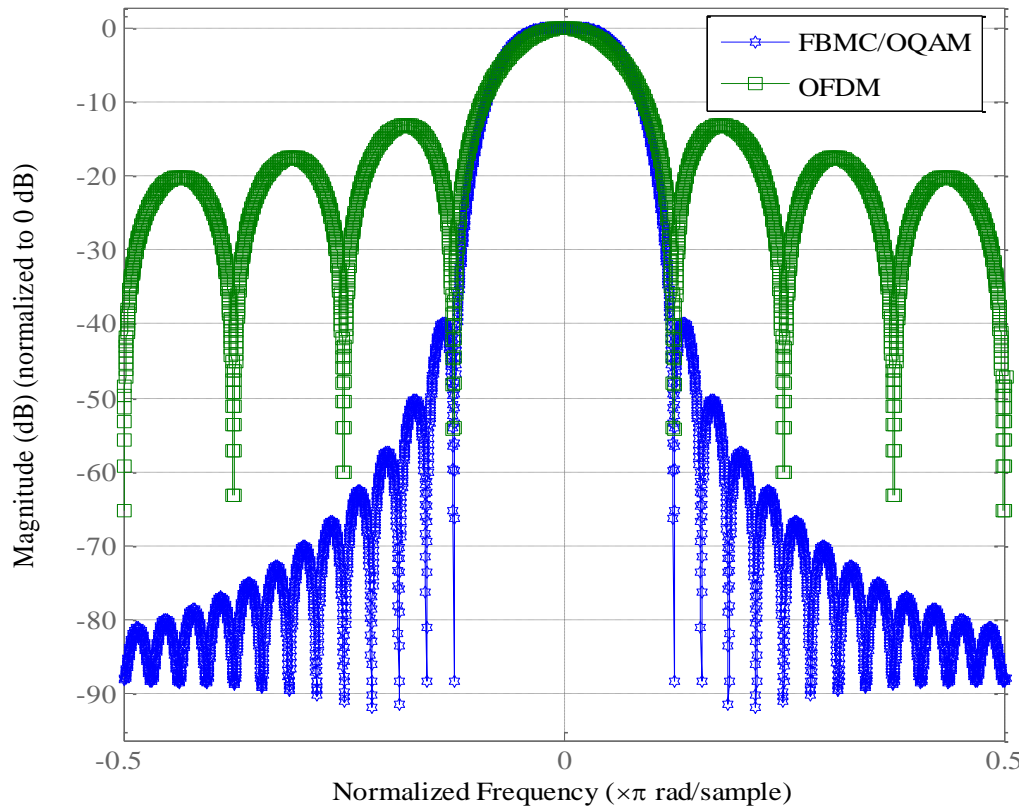
Figure 2.16: Frequency response of prototype filter for FBMC and OFDM.
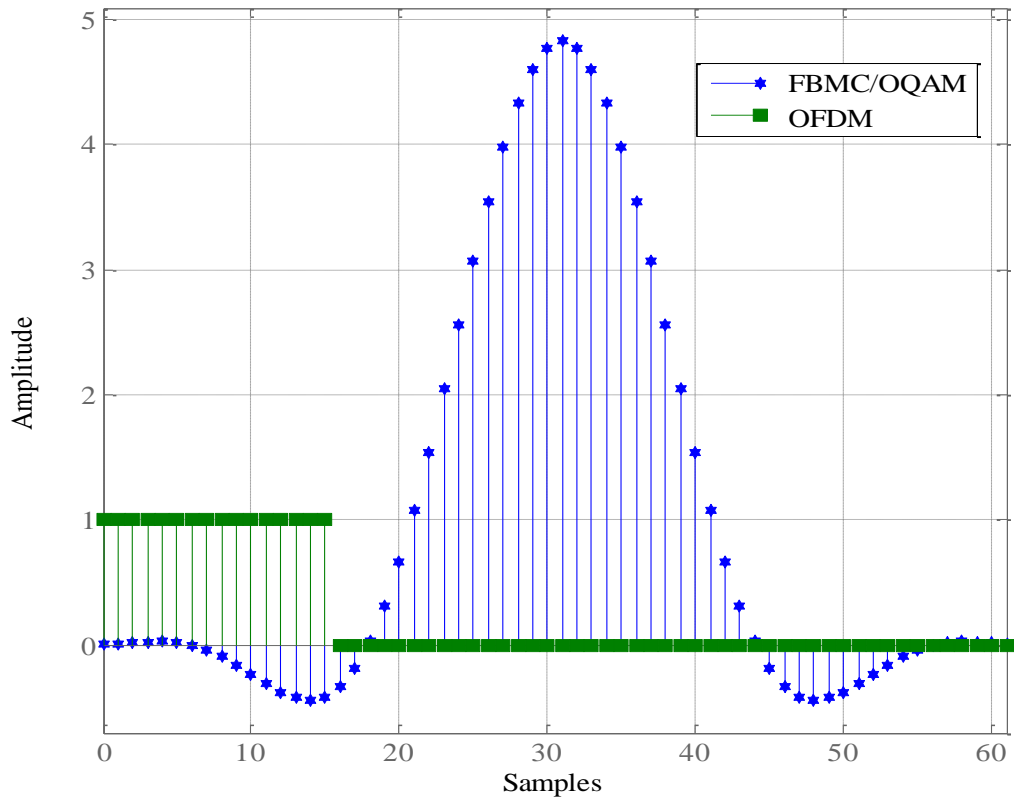
Figure 2.17: Impulse response of prototype filter for FBMC and OFDM.

Because of using well shaped prototype filter in FBMC, the side-lobe levels are considerably lower than in the case of OFDM. In this way, a good spectral containment for all the sub-channels can be obtained and this also results in a good resistance against narrowband interference as shown in Figure 2.18 and Figure 2.19. As a result, the bit error rate (BER) performance versus signal to noise ratio (SNR) for FBMC will be better than that for OFDM as shown in the Figure 2.20.
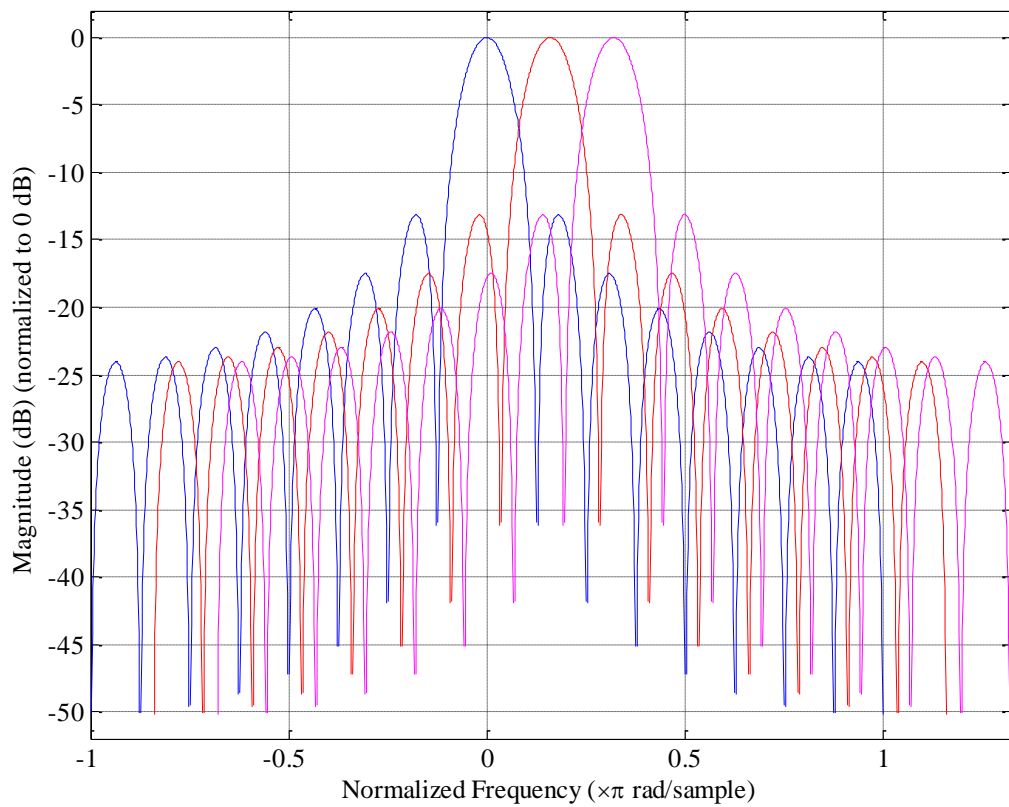
Figure 2.18: OFDM subcarriers.
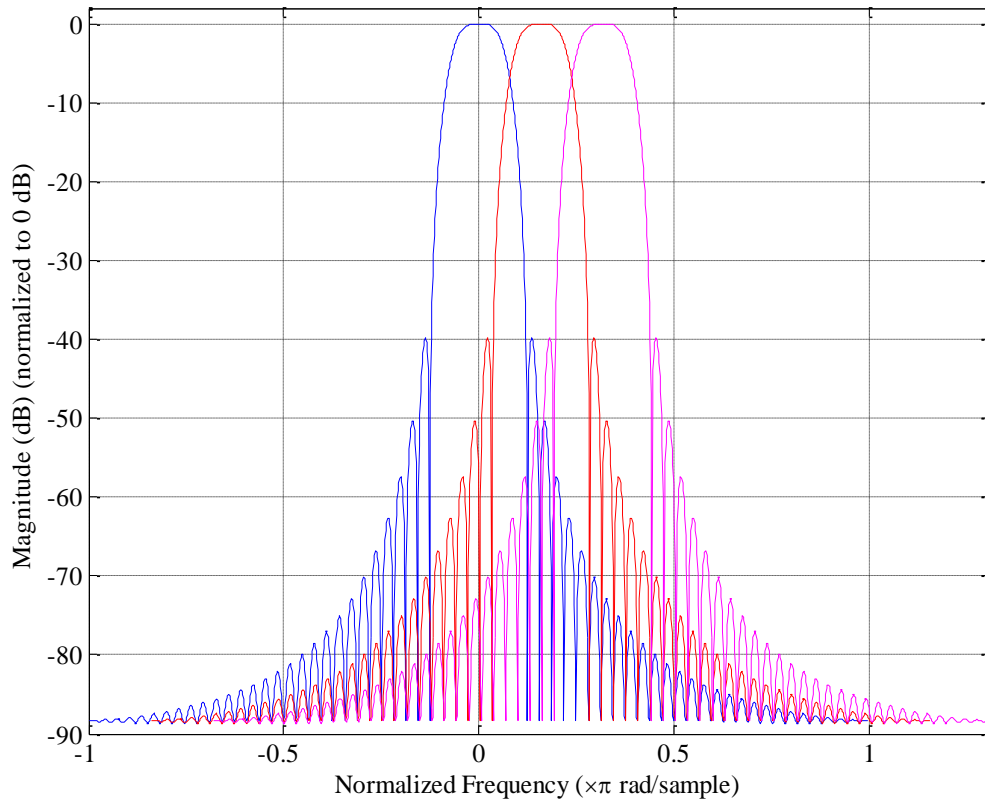
Figure 2.19: FBMC subcarriers.
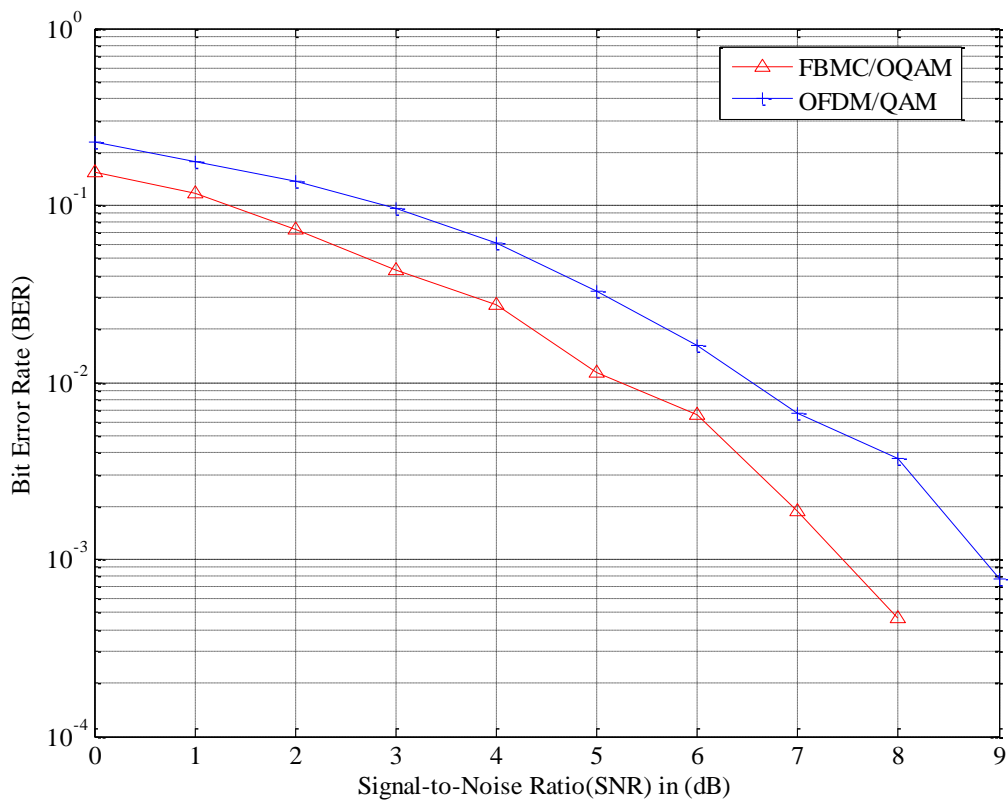
Figure 2.20: BER *vs* SNR performance comparison between FBMC and OFDM.

In fact, any sub-channel overlaps significantly only with its neighboring sub-channels. Then, in order to make two multicarrier signals independent, it is sufficient to leave an empty sub-channel between them.

Other advantages of FBMC over OFDM include better narrowband interference suppression capability and more bandwidth efficiency as no cyclic prefix is needed.

The computational complexity of FBMC system with polyphase implementation is greater than OFDM. Indeed, the complexity of OFDM system is dominated by the IFFT and FFT operations. Thus, the complexity of OFDM system can be written as:

$$O_{OFDM} = 2((\log_2(M) - 3) + 4) \tag{2.32}$$

The number of real multiplications as a function of number of sub-channels in the case of OFDM and FBMC are shown in the Figure 2.21:
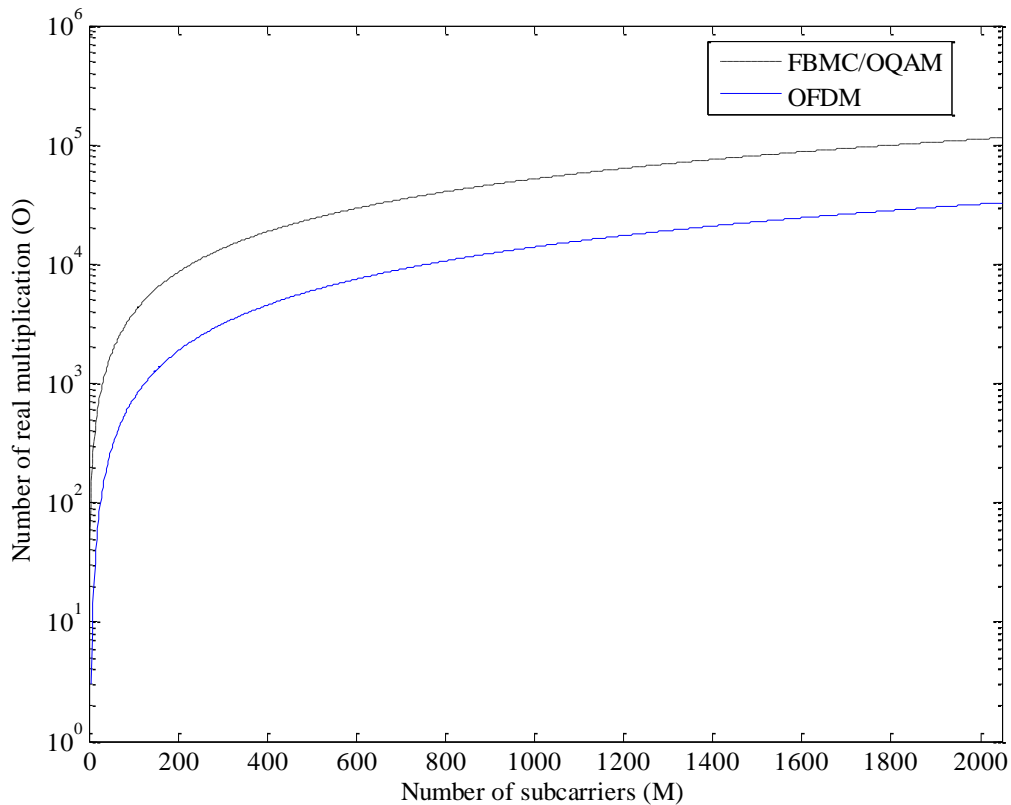
Figure 2.21: The number of real multiplications as a function of number of sub-channels for FBMC and OFDM.

Chapter 3

Fading Channel Estimation and

Equalization

3.1 State of the art

Many channel estimation techniques were proposed in the literature particularly for OFDM systems [Ozd07] [Col02] [Man01] [Che04] [Jam07]. They can be divided into training sequence/pilot symbols based techniques and blind techniques. The blind techniques require no training data. They utilize certain underlying mathematical information about the kind of data being transmitted. As blind techniques require a large amount of data, they are extremely computationally intensive and hence are impractical for real-system implementation. For this reason, we will focus our attention on the training sequence techniques in this thesis. The training sequence/pilot symbols based techniques are used in some existing mobile and wireless communication systems. The idea of training sequence/pilot symbols based techniques is that some portion of the transmitted signal is known to the receiver and used for channel estimation.

Compared to OFDM, the literature on FBMC/OQAM that addressed the problem of channel estimation and equalization are fairly limited [Lél08] [Kof13] [Kof11] [Sti10] [Lél12] [Ikh09] [Wal09]. In the FBMC/OQAM approach, the channel estimation issue is different of that in conventional OFDM. The reason is that, the sought channel frequency

response values are complex whereas the training input is real. Moreover, the AFB output samples also contain imaginary contributions from neighboring times and frequencies which is called intrinsic inter-symbol-interference. To reduce this intrinsic interference, under the assumptions of good time-frequency localization for the employed prototype filter and relatively low frequency selectivity for the channel, several methods are recently proposed, including both preamble-based [Lél08] [Kof13] [Kof11] and scattered pilots-based [Sti10] [Lél12] channel estimators.

In [Lél08] [Kof13] [Kof11], two preamble-based methods for channel estimation in FBMC/OQAM systems are presented. The first one is Pairs of Pilots (POP) technique [Lél08] shown in the Figure 3.1(a), which is based on the insertion of a pair of real-valued pilots at positions known by the receiver. In practice they can be placed at two consecutive time positions having the same subcarrier index. The second method is the Interference Approximation Method (IAM) which aims at approximating the intrinsic imaginary interference from neighboring pilots and hence constructing complex pilots, to accommodate the complex channel. It is based on the insertion of three pilots placed at three consecutive time positions having the same subcarrier index. The first and the third symbols have nonzero pilot while the middle pilot symbols are chosen so as to maximize the interference contributions from neighboring subcarriers. In [Kof13], a preamble structure called IAM-R signifies the presence of real pilots and IAM-C signifies the presence of complex (real/imaginary) pilots. These two structures are shown in Figure 3.1(b) and Figure 3.1(c), respectively. Another method [Kof11] extends IAM-C to incorporate side symbols as well. It is called Extended IAM-C (E-IAM-C) and is shown in Figure 3.1(d).
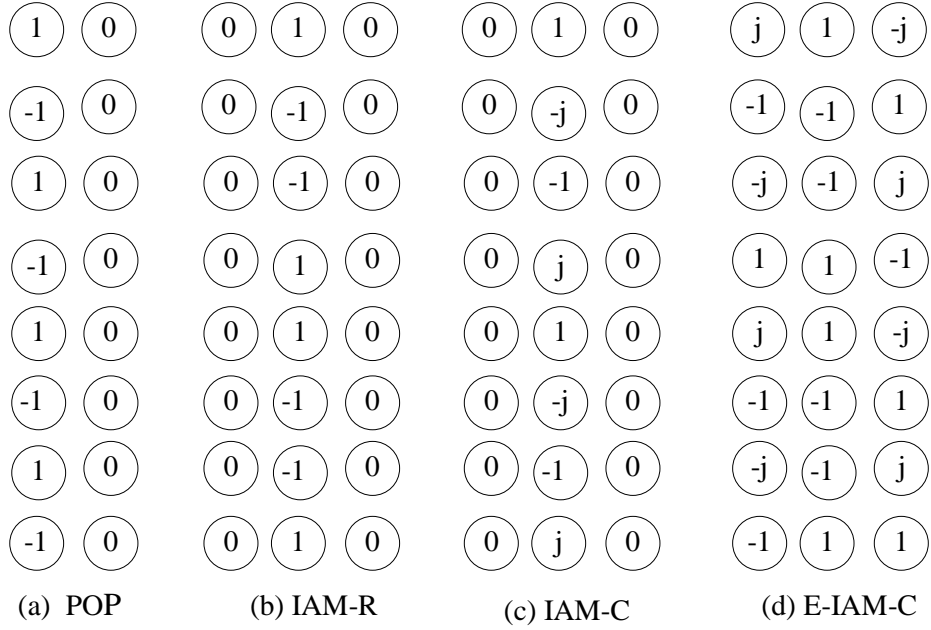
Figure 3.1: Preamble structures (POP, IAM-R, IAM-C and E-IAM-C).

In [Ikh09], a two stage MMSE equalizer is proposed to cope more efficiently with ICI. A fractionally spaced adaptive DFE based on the LMS algorithm was proposed in [Wal09] where the input of each equalizer comprises only the output of each subcarrier.

3.2 Pilot patterns

There are different types of pilot's arrangement that are used in OFDM channel estimation. The most famous types are block, comb and rectangular pilot patterns as shown in Figure 3.2. In block pilot pattern illustrated by Figure 3.2(a), OFDM channel estimation symbols are transmitted periodically, in which all subcarriers are used as pilots. The typical channel estimation methods for block pilot pattern are LS and MMSE. In comb pilot pattern illustrated by Figure 3.2(b), some of the subcarriers are reserved for pilots for each symbol. Figure 3.2(c) shows rectangular pilot pattern where OFDM blocks with comb pilots are sent periodically in a non continuous manner. In this thesis, we focus our attention on the comb pilot pattern.

(a) Block pilot pattern.

(b) Comb pilot pattern.

(c) Rectangular pilot pattern.
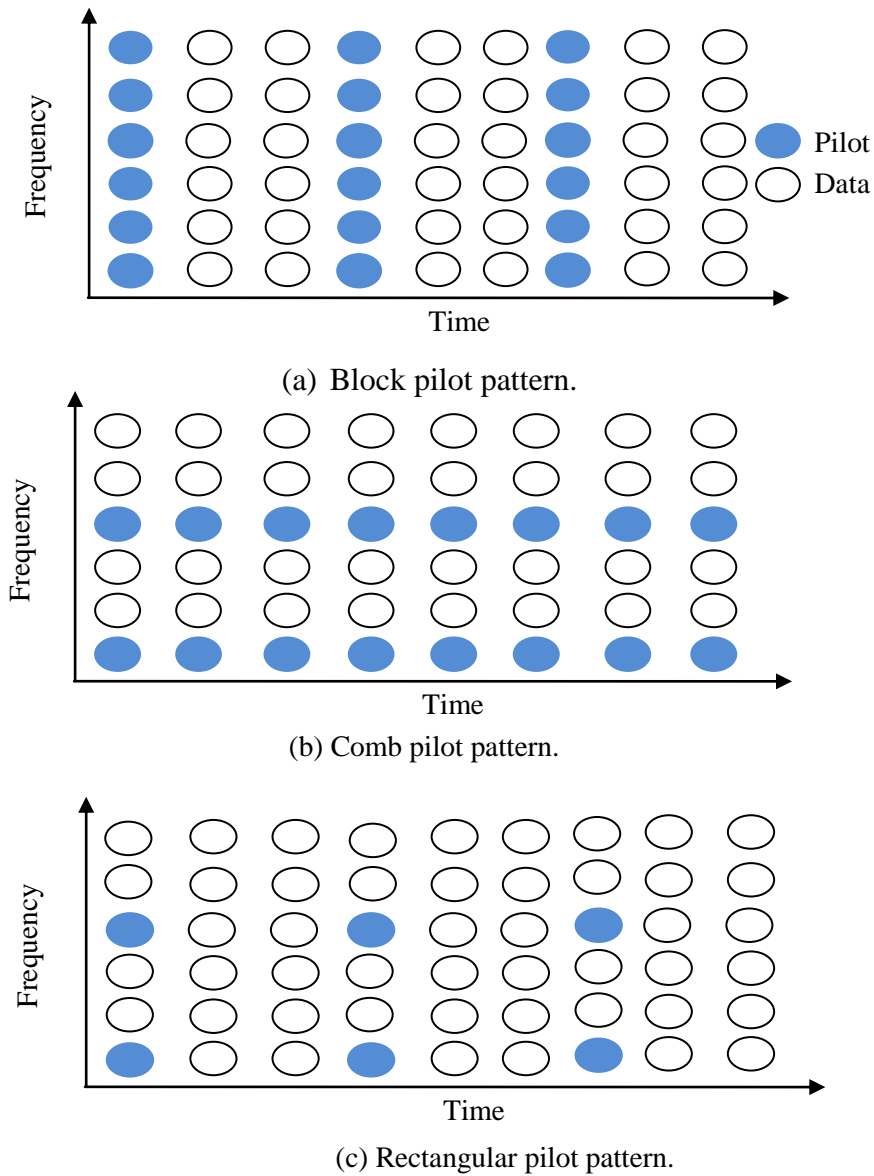
Figure 3.2: Pilot patterns.

3.3 Autoregressive channel modeling

Developing wireless channel models is important for channel simulator that replicates wireless channel data, and produces outputs that vary in a similar manner to the variations encountered in practice. There are different channel models such as sum-of-sinusoid simulation model [Jak74] and autoregressive model [Bad05]. The sum-of-sinusoid simulation model is an important model but this model is not practical for channel

estimation. On the other hand, the autoregressive model is simple, linear and contains few parameters that can be easily estimated.

To exploit the statistical properties of the fading channel given by its PSD and ACF, the fading process $h_k[n]$ can be modeled by a pth order AR process, denoted by AR(p) and defined as follows [Bad05]:

$$h_k[n] = -\sum_{i=1}^{p} a_i h_{k-i}[n] + v_k[n] \qquad (3.1)$$

where $\{a_i\}_{i=1,2,...,p}$ are the AR model parameters and $v_k[n]$ denotes a zero-mean complex white Gaussian driving process with equal variance σ_v^2 over all subcarriers. The PSD of the AR(p) process can be expressed as follows [Kay88]:

$$S(f_n) = \frac{\sigma_v^2}{\left|1 + \sum_1^p a_i e^{(-j2\pi f_n i)}\right|^2} \qquad (3.2)$$

where f_n is the normalized frequency.

The relationship between the AR parameters and the fading process auto-correlation function is given by the well-known Yule-Walker (YW) equations:

$$\boldsymbol{Ra} = -\boldsymbol{r} \qquad (3.3)$$

where $\boldsymbol{R}$ is the fading channel autocorrelation matrix defined by:

$$\boldsymbol{R} = \begin{bmatrix} r_0 & r_{-1} & \cdots & r_{-p+1} \\ r_1 & r_0 & \cdots & r_{-p+2} \\ \vdots & \vdots & \ddots & \vdots \\ r_{p-1} & r_{p-2} & \cdots & r_0 \end{bmatrix} \qquad (3.4)$$

$\boldsymbol{a}$ is the vector that contains the AR parameters as follows:

$$\boldsymbol{a} = \begin{bmatrix} a_1 \\ a_2 \\ \vdots \\ a_p \end{bmatrix} \qquad (3.5)$$

and

$$r = \begin{bmatrix} r_1 \\ r_2 \\ \vdots \\ r_p \end{bmatrix} \tag{3.6}$$

The variance of driving process σ_v^2 can be expressed as:

$$\sigma_v^2 = r_0 + \sum_{i=1}^{p} a_i r_{(-i)} \tag{3.7}$$

Choosing the order p is an important step in modeling the fading process using AR models. Baddour *et al.* [Bad05] use high order AR process (e.g., $p \geq 50$) when they simulate the channel. For this purpose, they modify the properties of the channel by considering the sum of the theoretical fading process and zero-mean white process whose variance is very small. Then, the AR parameters are estimated with the YW equations based on the modified autocorrelation function [Bad05]:

$$R_k^{mod} == J_0(2\pi f_d T_s |k|) + \varepsilon \delta_k \tag{3.8}$$

where ε is a very small bias used to overcome the ill conditioning of YW equations. It was observed in [Bad05] that the value of the added bias ε which results in the most accurate AR parameters computation depends mainly on the Doppler rate $f_d T_s$.

However, the computational complexity of the resulting channel estimation algorithm will also increase. Therefore, a compromise between the accuracy of the model and the computational complexity of the estimation algorithm has to be found. When the Doppler rate $f_d T_s$ is available at the receiver, the AR parameters $\{a_i\}_{i=1,2,\dots,p}$ can be computed by solving the YW equations. However, as the Doppler rate $f_d T_s$ is usually unknown, we propose to complete the joint estimation of the fading process $h_k[n]$ and its AR parameters $\{a_i\}_{i=1,2,\dots,p}$ based on dual Kalman filters that will be discussed in next sections.

3.4 Channel estimation

The estimation of the fading process $h_k[n]$ along the nth FBMC/OQAM symbol will be performed in two steps. Firstly, the fading process $h_k[n]$ at the pilot symbol position is estimated using LMS, RLS and dual Kalman filters. Secondly, the fading process at data symbol position will then be estimated by using some interpolation methods: linear, spline, or low-pass interpolation.

When using comb-type pilot arrangement [Col02] as shown in Figure 3.2(b), N_p pilots are uniformly inserted into $x_k[n]$ as follows:

$$x_k[n] = x_{uL+i}[n] = \begin{cases} x_{uL,pilot}[n], & i = 0 \\ x_{uL+i,data}[n], & i = 1, 2 \cdots, L-1 \end{cases} \qquad (3.9)$$

where $x_{uL,pilot}[n]$ is the uth pilot symbol with $u = 0,1, \dots, N_p - 1$, and $L = M/N_p$ is the pilot interval spacing with M is the number of subcarriers.

3.4.1 Fading process estimation at pilot symbol positions

In this subsection, our purpose is to estimate the fading process $h_k[n]$ over the nth FBMC/OQAM symbol based on adaptive filters (LMS, RLS and Dual kalman filters) with known pilot symbols. Note that, for the sake of simplicity and clarity of presentation, the time index is dropped. Thus, the fading process $h_k[n]$ is reduced to h_k.

3.4.1.1 Dual Kalman filters

We propose to jointly estimate the fading process $h_k[n]$ and its AR parameters $\{a_i\}_{i=1,2,\dots,p}$ based on dual Kalman filters as shown in Figure 3.3. Indeed, the first Kalman filter in Figure 3.3 uses the pilot symbol $x_{k,pilot}[n]$, the output of the analysis filter bank $s_k[n]$ and the latest estimated AR parameters $\{\hat{a}_i\}_{i=1,2,\dots,p}$ to estimate the fading process $h_k[n]$; while

the second Kalman filter uses the estimated fading process $\hat{h}_k[n]$ to update the AR parameters.
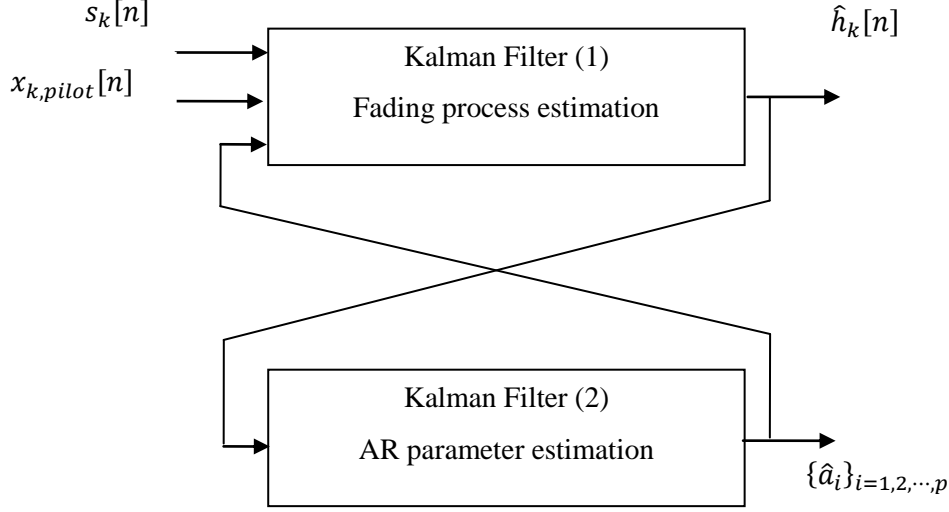
Figure 3.3: Dual Kalman filters based structure for the joint estimation of the fading process and its AR parameters over the nth FBMC/OQAM symbol.

3.4.1.2 Fading process estimation

Our purpose is to estimate the fading process $h_k[n]$ over the nth FBMC/OQAM symbol based on Kalman filtering with known pilot symbols. To this end, let us define the state vector as follows:

$$\boldsymbol{h}_k = \begin{bmatrix} h_k & h_{k-1} & \dots h_{k-p+1} \end{bmatrix}^T \tag{3.10}$$

Then, equation (3.1) can be written in the following state-space form:

$$\boldsymbol{h}_k = \boldsymbol{\phi} \boldsymbol{h}_{k-1} + \boldsymbol{g} v_k \tag{3.11}$$

where:

$$\boldsymbol{\phi} = \begin{bmatrix} -a_1 & -a_2 & \cdots & -a_p \\ 1 & 0 & \cdots & 0 \\ \vdots & \vdots & \ddots & \vdots \\ 0 & \cdots & 1 & 0 \end{bmatrix} \text{ is the transition matrix and } \boldsymbol{g} = \begin{bmatrix} 1 & 0 & \dots 0 \end{bmatrix}^T \tag{3.12}$$

In addition, given equations (3.11) and (2.32), it follows that:

$$s_k = x_k^T h_k + \eta_k \tag{3.13}$$

where $x_k = [\, x_{k,pilot} \quad 0 \quad \cdots \quad 0 \,]^T$

Hence, equations (3.11) and (3.13) represent the state-space model dedicated to the nth FBMC/OQAM symbol fading channel system (2.31) and (3.1). A standard Kalman filtering algorithm can then be carried out to provide the estimation $\widehat{h}_{k/k}$ of the state vector h_k given the set of observations $\{s_i\}_{i=0,\cdots,M-1}$. To this end, let us introduce the so-called innovation process α_k which can be obtained as follows:

$$\alpha_k = s_k - x_k^T \phi \widehat{h}_{k-1/k-1} \tag{3.14}$$

The variance of the innovation process can be expressed as:

$$C_k = E[\alpha_k \alpha_k^*] = x_k^T P_{k/k-1} x_k + \sigma_{\eta_k}^2 \tag{3.15}$$

where the so-called *a priori* error covariance matrix $P_{k/k-1}$ can be recursively obtained as follows:

$$P_{k/k-1} = \phi P_{k-1/k-1} \phi^H + g\sigma_v^2 g^T \tag{3.16}$$

The Kalman gain is calculated in the following manner:

$$K_k = P_{k/k-1} x_k C_k^{-1} \tag{3.17}$$

The *a posteriori* estimate of the state vector and the fading process are, respectively, given by:

$$\widehat{h}_{k/k} = \phi \widehat{h}_{k-1/k-1} + K_k \, \alpha_k \tag{3.18}$$

and

$$\hat{h}_k = \hat{h}_{k/k} = g^T \widehat{h}_{k/k} \tag{3.19}$$

The error covariance matrix is updated as follows:

$$P_{k/k} = P_{k/k-1} - K_k x_k^T P_{k/k-1} \tag{3.20}$$

It should be noted that the state vector and the error covariance matrix are initially assigned to zero vector and identity matrix respectively, i.e. $\widehat{h}_{0/0} = 0$ and $P_{0/0} = I_p$.

Equations (3.14)-(3.20) can be evaluated providing the availability of the AR parameters that are involved in the transition matrix ϕ and the driving process variance σ_v^2. They will be estimated in the next subsections.

3.4.1.3 Estimation of the AR parameters

To estimate the AR parameters from the estimated fading process $\widehat{h}_k$, equations (3.218) and (3.19) are firstly combined such as the estimated fading process is a function of the AR parameters:

$$\widehat{h}_k = g^T \phi \widehat{h}_{k-1} + g^T K_k \alpha_k = \widehat{h}_{k-1}^T a_k + \varsigma_k \tag{3.21}$$

where $\widehat{h}_{k-1} = [\ \widehat{h}_{k-1}\ \ \widehat{h}_{k-2}\ \ \cdots\ \ \widehat{h}_{k-p}]$, and $a_k = [\ -a_1\ \ -a_2\ \ \cdots\ \ -a_p]^T$. In addition, the variance of the process $\varsigma_k = g^T K_k \alpha_k$ is given by:

$$\sigma_{\varsigma_k}^2 = g^T K_k C_k K_k^H g \tag{3.22}$$

When the channel is assumed stationary, the AR parameters are invariant and satisfy the following relationship:

$$a_k = a_{k-1} \tag{3.23}$$

As equations (3.21) and (3.23) define a state-space representation for the estimation of the AR parameters, a second Kalman filter can be used to recursively estimate a_k as follows:

$$\widehat{a}_k = \widehat{a}_{k-1} + K_{a_k}(\widehat{h}_k - \widehat{h}_{k-1}^T \widehat{a}_{k-1}) \tag{3.24}$$

where the Kalman gain K_{a_k} and the update of the error covariance matrix P_a are, respectively, given by:

$$K_{a_k} = P_{a_{k-1}} \widehat{h}_{k-1}^* \left(\widehat{h}_{k-1}^H P_{a_{k-1}} \widehat{h}_{k-1} + \sigma_{\varsigma_k}^2 \right)^{-1} \tag{3.25}$$

and

$$P_{a_k} = P_{a_{k-1}} - K_{a_k} \widehat{h}_{k-1}^T P_{a_{k-1}} \tag{3.26}$$

with initial conditions $\widehat{a}_0 = 0$ and $P_{a_0} = I_p$.

3.4.1.4 Estimation of the driving process variance

To estimate the driving process variance $\sigma_v{}^2$, the Riccati equation is first obtained by inserting (3.16) in (3.20) as follows:

$$P_{k/k} = \phi P_{k-1/k-1} \phi^H + g \sigma_{v_k}^2 g^T - K_k x_k^T P_{k/k-1} \tag{3.27}$$

Taking into account that $P_{k/k-1}$ is a symmetric Hermitian matrix, one can rewrite (3.21) in the following manner:

$$b_k^T P_{k/k-1} = C_k K_k^H \tag{3.28}$$

By combining (3.31) and (3.32), σ_v^2 can be expressed as follows:

$$\sigma_v^2 = f \left[P_{k/k} - \phi P_{k-1/k-1} \phi^H + K_k C_k K_k^H \right] f^T \tag{3.29}$$

where $f = [g^T g]^{-1} g^T = g^T$ is the pseudo-inverse of g.

Thus, σ_v^2 can be estimated recursively as follows:

$$\widehat{\sigma}_{v\,k}^2 = \lambda \sigma_{v\,k-1}^2 + [1 - \lambda] f \left[P_{k/k} - \phi P_{k-1/k-1} \phi^H + K_k |\alpha_k|^2 K_k^H \right] f^T \tag{3.30}$$

where the variance of the innovation process C_k is replaced by its instantaneous value $|\alpha_k|^2$ and λ is the forgetting factor. It should be noted that λ can be either constant or subcarrier-varying (e.g., $\lambda_k = (k - 1)/k$).

3.4.2 Fading process estimation at data symbol positions

Once the fading process at pilot symbol positions are estimated by the various channel estimators, the fading process at data symbol positions will then be estimated by using some interpolation methods such as linear, spline, or low pass interpolation [Col02].

3.4.2.1 Linear interpolation

Using linear interpolation method, the channel estimates at data positions, $uL < k < (u+1)L$, is given by:

$$\hat{h}_k = \left(\hat{h}_{p_{k+1}} - \hat{h}_{p_k}\right)\frac{l}{L} + \hat{h}_{p_k}, \qquad 0 \le l < L \qquad\qquad (3.31)$$

where $\hat{h}_{p_k}$ is the estimated fading process at pilot symbol position.

3.4.2.2 Low-pass interpolation

The low-pass interpolation is carried out by inserting zeros into the data symbol positions of the original sequence and then applying a special low-pass filter. In this thesis, we use the Matlab function *interp.*

3.4.2.3 Spline interpolation

Spline interpolation produces a smooth and continuous polynomial fitted to the estimated fading process at pilot symbol positions. In this thesis, we use the Matlab function *spline.*

3.4.3 Fading channel equalization

Once the fading process at pilot and data symbols are estimated using the proposed approach, channel equalization can be performed by multiplying equation (2.31) with a normalized version of the complex conjugate of the channel estimate as follows:

$$\hat{x}_k[n] = s_k[n] \left(\frac{\hat{h}_k^*[n]}{\left|\hat{h}_k[n]\right|^2} \right) \tag{3.32}$$

Chapter 4

Simulation Results

4.1 Simulation environment

In this chapter, we carry out a comparative simulation study on the estimation of FBMC/OQAM fading channels between the dual Kalman filters based channel estimator and the conventional LMS and RLS channel estimators. In addition, we test the performance of three interpolation techniques; namely: low-pass, spline and linear interpolation. Furthermore, we investigate the effect of the number of pilot symbols N_p and Doppler rate $f_d T_s$ on the BER performance. The FBMC/OQAM wireless system is implemented and simulated using MATLAB to allow various parameters of the system to be varied and tested.

In all of our simulations, the fading channels are generated according to the autoregressive model based method presented in [Bad05]. The autoregressive model order p in the dual Kalman filters based estimator is set to $p = 2$ [Has06]. The step size for the LMS algorithm is set to $\mu = 0.5$ [Gel99] and the forgetting factor for RLS algorithm is set to $\lambda = 0.1$ [Cio09].

4.2 Estimated fading process

In this section we want to study the envelope of estimated fading process in the cases of using different adaptive filters and using various interpolation methods. In addition, we want to present the estimated parameters of the fading process. In our simulation we use SNR=15 dB, $M = 2048$, $N_p = 1024$, and $f_d T_s = 0.0167$.

4.2.1 Estimated envelope of the fading process

Figure 4.1 shows the envelope of estimated fading process using the various channel estimators with low-pass interpolation. We can notice that the dual Kalman filters based estimator provides better estimation than the LMS and RLS based ones particularly at deep fading.
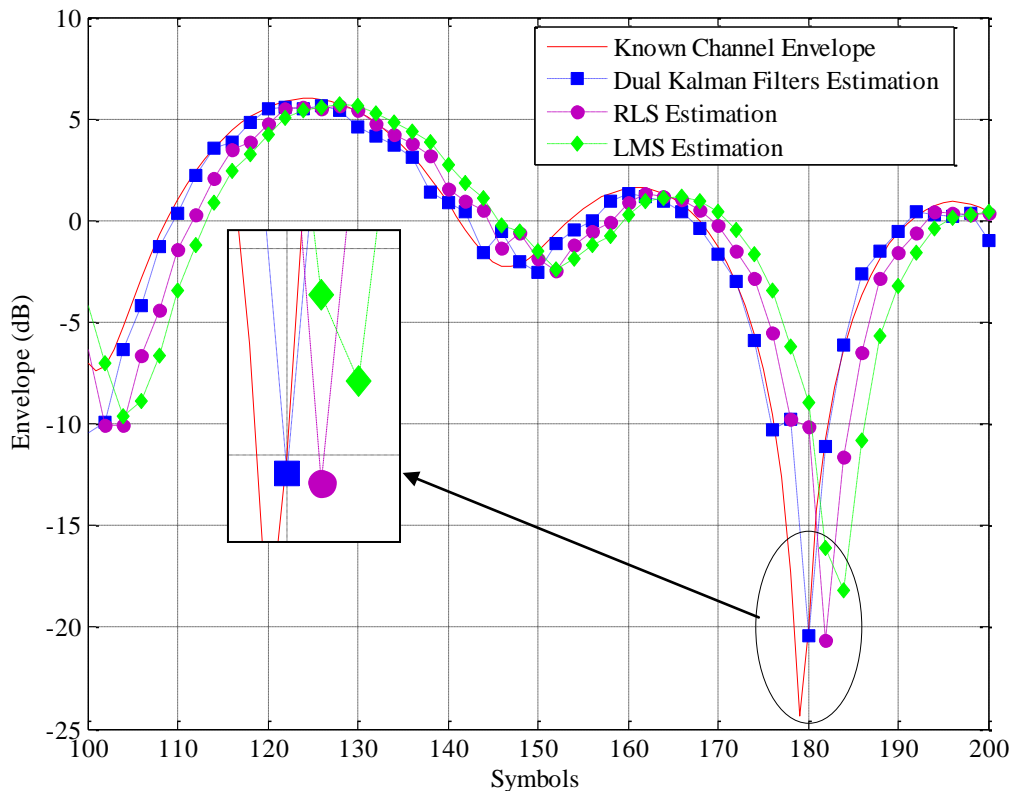
Figure 4.1: Envelope of estimated fading process using the various estimators SNR=15 dB, M=2048, N_p=1024, and $f_d T_s$ =0.0167.

Figure 4.2 illustrate the envelope of estimated fading process using dual Kalman filters with various interpolation methods. We can notice that the low-pass interpolation provides better estimation than spline and linear interpolation.
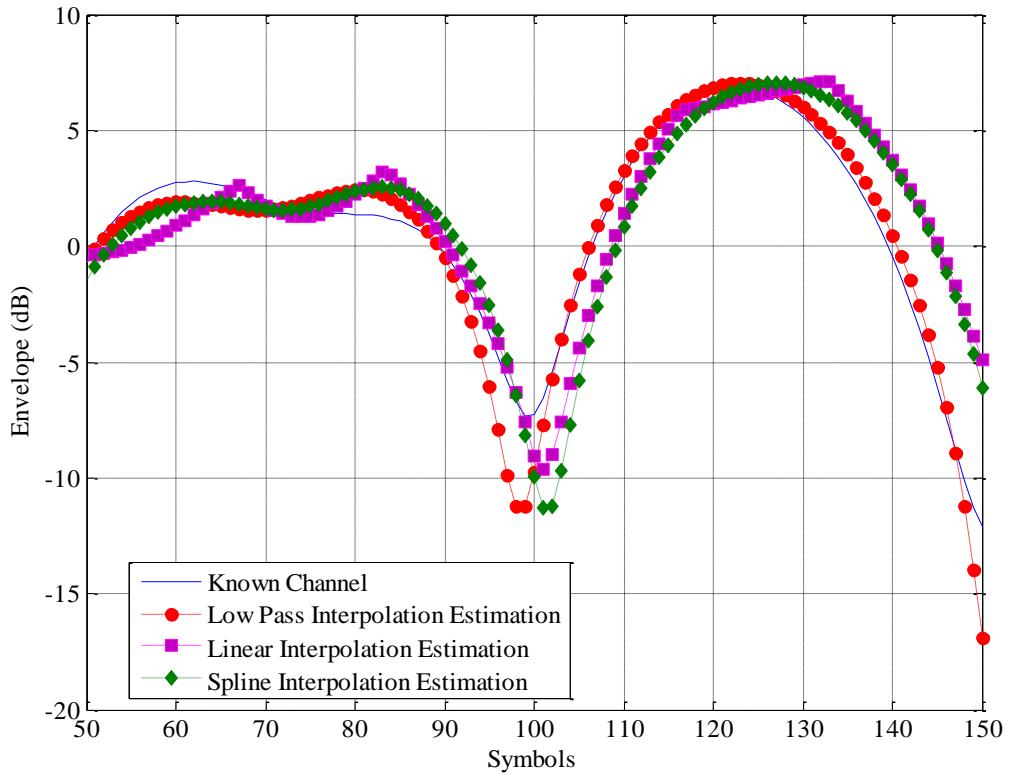
Figure 4.2: Envelope of estimated fading process using dual Kalman filters with the various interpolation methods. SNR=15 dB, M=2048, N_p=256, and $f_d T_s$ =0.0167.

4.2.2 Estimated parameters of the fading process

Figure 4.3 shows the real and imaginary parts of the estimated AR(2) parameters of the fading process and the driving process variance using dual Kalman filters. The true values of AR(2) parameters are $a_1 = -1.9931$, $a_2 = 0.9986$ and $\sigma_v^2 = 1.504 \times 10^{-5}$. One can notice that the estimated real and imaginary parts of the AR(2) parameters converge to the true values.
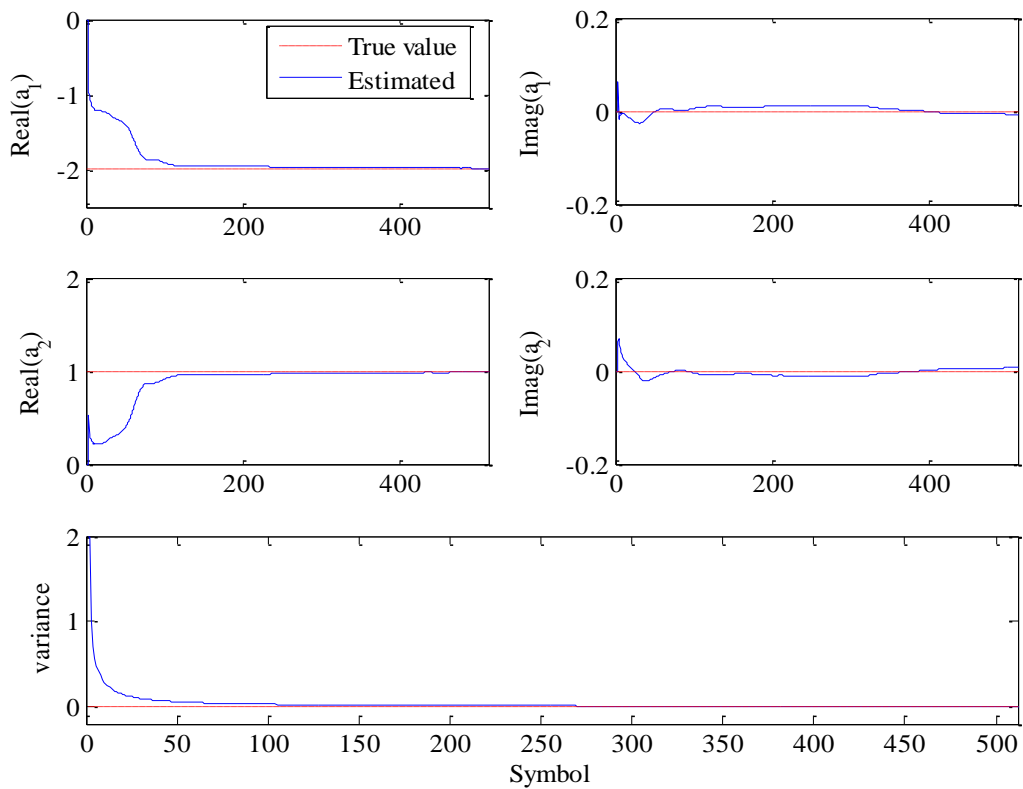
Figure 4.3: Estimation of the AR(2) parameters and the driving process variance using Dual Kalman filters. True values are $a_1 = -1.9931$, $a_2 = 0.9986$ and $\sigma_v^2 = 1.504 \times 10^{-5}$. *SNR*=15 dB, $M = 2048$, $N_p = 1024$, *and* $f_d T_s = 0.0167$.

4.3 BER performance versus SNR

Here we want to study the BER performance versus SNR in the cases of different adaptive filters, changing the number of pilots and using various interpolation methods.

Figure 4.4 displays the BER performance versus SNR for the FBMC/OQAM system when using the various channel estimators with $M = 2048$, $N_p = 1024$ pilots, $f_d T_s = 0.0167$, and using low-pass interpolation. According to Figure 4.4, the proposed dual Kalman filters based estimator outperforms the conventional LMS and RLS estimators with the performance difference increases as the SNR increases.
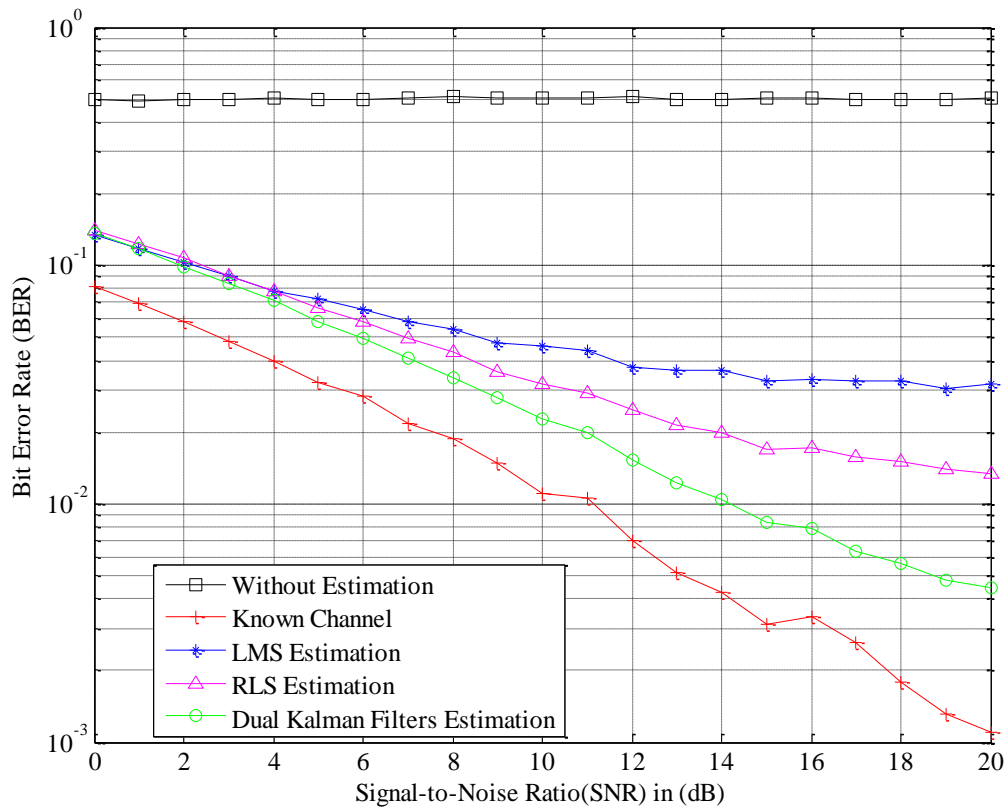
Figure 4.4: BER performance versus SNR for the FBMC/OQAM system with the various channel estimators. M=2048,N_p=1024,and $f_d T_s$ =0.0167.

Figure 4.5 shows the effect of changing the number of pilot symbols N_p on the BER performance of the FBMC/OQAM system when using dual Kalman filters based channel estimator with low-pass interpolation. Indeed, increasing the number of pilot symbols N_p will improve the BER performance of the system.
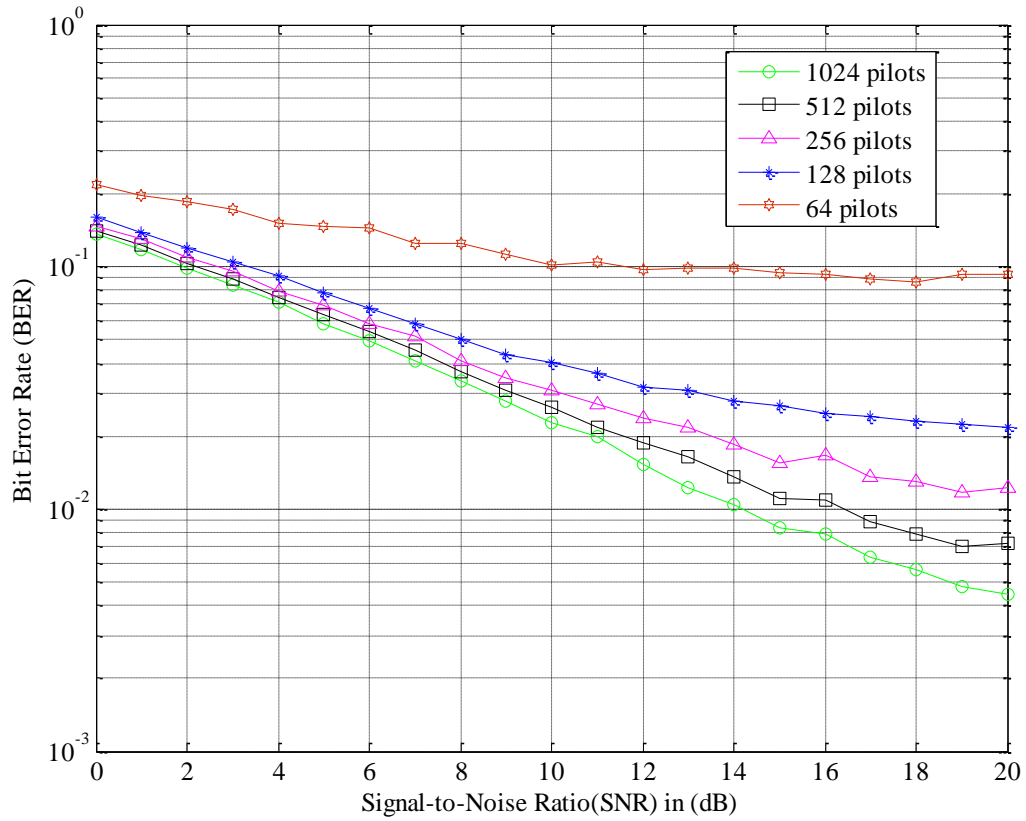
Figure 4.5: BER performance versus SNR for the FBMC/OQAM system with different number of pilot symbols. M=2048, $f_d T_s$ =0.0167.

Figure 4.6 displays the BER performance of the FBMC/OQAM system when using dual Kalman filters with the various interpolation Methods, $M = 2048$, $N_p = 256$ pilots, and $f_d T_s = 0.0167$. It is confirmed that the low-pass interpolation yields the best BER performance.
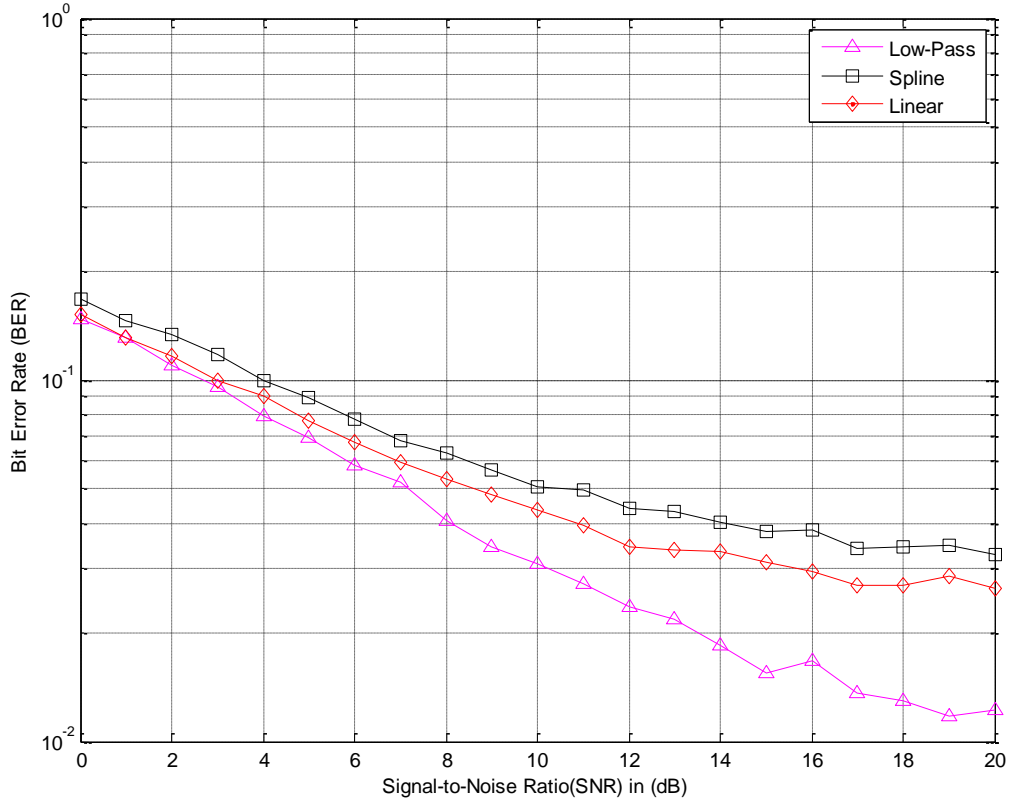
Figure 4.6: BER performance versus SNR for the FBMC/OQAM system with the various interpolation methods. M=2048, N_p=256, and $f_d T_s$=0.0167.

4.4 BER performance versus Doppler rate

In this section we study the effect of Doppler rate on the BER performance in the cases of different adaptive filters and different values of SNR.

Figure 4.7 displays the BER performance of the FBMC/OQAM system versus Doppler rate when using the various channel estimators with low-pass interpolation, $M = 2048$, $N_p = 1024$ pilots. One can notice that the dual Kalman filters based estimator yields lower

BER performance than the LMS and RLS estimators with the BER performance difference increases as the Doppler rate increases. This confirms that the dual Kalman filters based estimator can exploit the fading channel statistics and can track fast variations of rapidly varying fading channels.
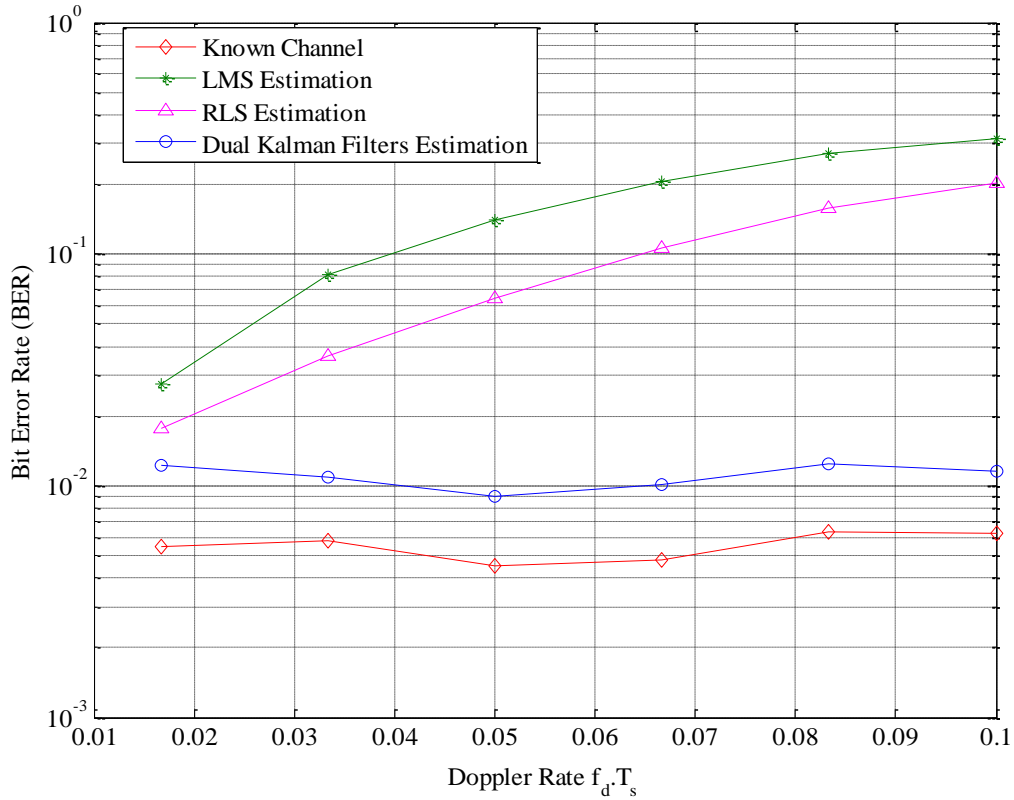
Figure 4.7: BER performance versus Doppler rate for the FBMC/OQAM system with the various channel estimators. SNR=15dB, M=2048 and N_p=1024.

Figure 4.8 shows the BER performance of the FBMC/OQAM system versus Doppler rate when using dual Kalman filters with low-pass interpolation and different SNR, $M = 2048$, $N_p = 1024$ pilots. One can notice that the BER performance will be better when increasing SNR.
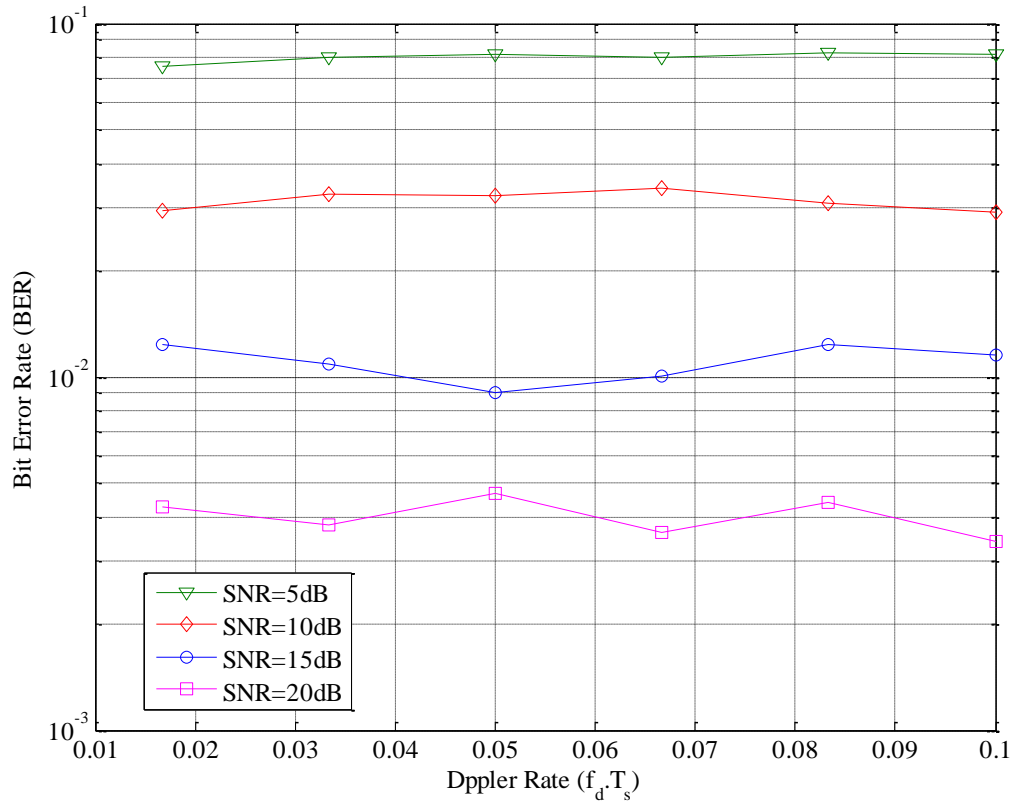
Figure 4.8: BER performance versus Doppler rate of the FBMC/OQAM system using dual Kalman filters with low pass interpolation, different SNR, M=2048 and N_p=1024.

Chapter 5

Conclusion and Future Work

5.1 Conclusion

FBMC is currently more attractive than OFDM for different communication systems applications. Indeed, it has several advantages over OFDM. Firstly, it does not require CP which gives better usage of the allocated spectrum. In addition, it has a prototype filter designed under Nyquist criteria which can reduce the spectral leakage problem of OFDM and hence reducing the ISI and ICI. Moreover, when filter banks are combined with offset quadrature amplitude modulation (FBMC/OQAM), this will lead to a maximum data transmission rate.

We address the estimation and equalization of FBMC/OQAM fading channels based on pilot symbols. The relevance of the dual Kalman filters based structure is studied for the joint estimation of the fading process and its AR parameters over each subcarrier at pilot symbol positions. The fading process at data symbol positions is then obtained by using some interpolation methods such as linear, spline, or low-pass interpolation. The simulation results showed that the dual Kalman filters based estimator outperforms the LMS and RLS based ones. Indeed, the dual Kalman filters based estimator can exploit the fading channel statistics and can track fast variations of rapidly varying fading channels. In addition, the low-pass interpolation is confirmed to outperform both spline and linear interpolation.

5.2 Future Work

At the end of this thesis, several problems can be suggested for future work. They can be pointed out as below:

- We have assumed that the fading processes over all carriers are uncorrelated and, hence, they are estimated separately. However, correlation among multi-carrier fading processes might arise due to the existence of a significant Doppler spread for instance [Kal13]. To exploit these correlations, the joint estimation of the fading processes can be addressed based on a vector (multi-channel) AR model. Therefore, the extension of the proposed channel estimation techniques to account for a vector AR model is a possible direction for future work [Jam11].

- We have used only comb-pilot arrangement for channel estimation. Possible future work can investigate the relevance of other pilot arrangements such as block or rectangular pilot arrangements for channel estimation [Col02].

- Instead of the dual Kalman filters, we can investigate the relevance of the dual H∞ filters for the joint estimation of the channel fading coefficients and their corresponding AR parameters [Jam11].

Acronyms and Abbreviation

ACF: Auto-Correlation Function

AFB: Analysis Filter Bank

AR: Auto-Regressive

AWGN: Additive White Gaussian Noise

BER: Bit Error Rate

CMT: Cosine Modulated Multitone

CP: Cyclic Prefix

DAB: Digital Audio Broadcasting

DFE: Decision Feedback Equalizer

DSL: Digital Subcarrier Line

DVB: Digital Video Broadcasting

DWMT: Discrete Wavelet Multitone

EMFB: Exponentially Modulated Filter Bank

FBMC: Filter Bank Multicarrier

FFT: Fast Fourier Transform

FIR: Finite Impulse Response

FMT: Filtered Multi-Tone

IAM: Interference Approximation Method

ICI: Inter-Carrier Interference

IFFT: Inverse Fast Fourier Transform

ISI: Inter-Symbol Interference

LMS: Least Mean Square

LS: Least Square

LTE: Long Term Evolution

MC: Multi-Carrier

MC-CDMA: Multi-Carrier Code Division Multiple Access

MDFT: Modified Discrete Fourier Transform

MMSE: Minimum Mean Square Error

MSE: Mean Square Error

NPR: Nearly Perfect Reconstruction

OFDM: Orthogonal Frequency Division Multiplexing

OQAM: Offset Quadrature Amplitude Modulation

PAM: Pulse Amplitude Modulation

POP: Pairs Of Pilots

PR: Perfect Reconstruction

PSD: Power Spectrum Density

QAM: Quadrature Amplitude Modulation

RLS: Recursive Least Square

SFB: Synthesis Filter Bank

WiMAX: Worldwide interoperability for Microwave Access

WLAN: Wireless Local Area Networks

YW: Yule-Walker

Notations

$a_k[m]$: Synthesis polyphase filter at the transmitter in time index

$b_k[m]$: Analysis filter polyphase at the receiver in time index

$c_k[l]$: QAM complex valued symbol

$f_d T_s$: Doppler rate

f_d: Doppler frequency

$F_k(z)$: Analysis filter transfer function for sub-channel k

$f_k[m]$: Analysis filter impulse response for sub-channel k

f_s: Sampling rate (at SFB output and AFB input

g_{kl}: Random scatterer amplitude

$G_k(z)$: Synthesis filter transfer function for sub-channel k

$g_k[m]$: Synthesis filter impulse response for sub-channel k

$\hat{h}_k[n]$: Estimated fading channel

$h_k[n]$: Fading channel along subcarriers at symbol n

$J_0(.)$: Zero order Bessel function

k : Subcarrier index (k=0, …, M-1; k=0 corresponds to center subcarrier)

K: Overlapping factor in prototype filter design

$\boldsymbol{K}_{a_k}$: Kalman gain

l : Sample index at OQAM pre-processing input/post-processing output

L_p: Prototype filter length

L_s: Number of scatters

m : Sample index at SFB output/AFB input

M: Overall number of subcarriers, FFT size

n : Sample index at OQAM pre-processing output/post-processing input

N_p: Number of pilot symbols

$p[m]$: Discrete time of prototype filter impulse response

$\boldsymbol{P_a}$: Error covariance matrix

R : Fading channel autocorrelation matrix

$r[m]$: Received signal

R_k: Autocorrelation function

$S(f)$: Power spectrum density function

$s_k[n]$: Signal at the input of channel estimation and equalization

T_s: Sampling interval (at SFB output and AFB input)

v : Mobile speed

$w_k[m]$: AWGN signal

$y[m]$: Transmitted signal

$\beta_k[n]$: Multipliers

ϑ_{kl} : Initial phase

$\theta_k[n]$: Phase mapping between real data sequence and complex samples at the SFB input

λ : Forgetting factor of RLS

μ: LMS step size

$\boldsymbol{\phi}$: Transition matrix

φ_{kl}: Angle of arrival

Bibliography

[Ald13]   Mahmoud Aldababseh and Ali Jamoos, "Estimation of FBMC/OQAM Fading Channels Using Dual Kalman Filters," submitted to Wireless Personal Communications Journal, Springer, March 2013.

[Alh03]   J. Alhava and M. Renfors, "Exponentially-modulated filter bank-based transmultiplexer," in Proc. IEEE Int. Symp. Circuits and Systems, Bangkok, Thailand, May 2003, vol. IV, pp. 233-236.

[Bad05]   K. E. Baddour and N. C. Beaulieu, "Autoregressive modeling for fading channel simulation," IEEE Trans. On Wireless Commun., vol. 4, no. 4, pp. 1650-1662, July 2005.

[Beh11]   Behrouz Farhang-Boroujeny, "OFDM versus filter bank multicarrier", IEEE Signal Processing Magazine, vol. 28, pp. 92-112, 2011.

[Bel01]   M. G. Bellanger, "Specification and design of a prototype filter for filter bank based multicarrier transmission," in Proc. IEEE Int. Conf. Acoustics, Speech, and Signal Processing, Salt Lake City, USA, pp. 2417-2420, May 2001.

[Bel09]   M. Bellanger, "Prototype filter and filter bank structure", Technical Report, PHYDYAS Project, 2009.

[Che00]   G. Cherubini, E. Eleftheriou, S. Olcer, and J. M. Cioffi, "Filter bank modulation techniques for very high-speed digital subscriber lines," IEEE Commun. Mag., pp. 98-104, May 2000.

[Che04]   W. Chen and R. Zhang, "Estimation of time and frequency selective channels in OFDM systems: a Kalman filter structure," in Proc. IEEE GLOBECOM'04, pp. 800-803, Nov. 2004.

[Cio09]   S. Ciochina, C. Paleologu, J. Benesty, A. A. Enescu, "On the influence of the forgetting factor of the RLS adaptive filter in system identification", International Symposium on Signals, Circuits and Systems - ISSCS, July 2009. doi: 10.1109/ISSCS.2009.5206117.

[Col02]   S. Coleri, M. Ergen, A. Puri, and A. Bahai, "Channel estimation techniques based on pilot arrangement in OFDM systems," IEEE Trans. Broadcast., vol. 48, no. 3, pp. 223–229, Sept. 2002.

[Gel99]   S. Gelfand, Y. Wei, and J . Krogmeier, "The Stability of Variable Step-Size LMS Algorithms", IEEE TRANSACTIONS ON SIGNAL PROCESSING, vol. 47, no. 12, Dec. 1999.

[Has06]   W. Hassasneh, A. Jamoos, E. Grivel and H. Abdel Nour, "Estimation of MC-DS-CDMA Fading Channels Based on Kalman Filtering with High Order Autoregressive Models, " in proceedings of the Mobile Computing and Wireless Communications international conference (IEEE MCWC2006), Amman-Jordan, September 17-20, 2006.

[Ikh09]   A. Ikhlef and J. Louveaux, "An Enhanced MMSE Per Subchannel Equalizer For Highly Frequency Selective Channels for FBMC Systems," in Proc. IEEE-SPAWC'09, Perugia, 22-24 June 2009.

[Jakes74]   W. C. Jakes, Microwave Mobile Communications. New York: Wiley, 1974.

[Jam07]   A. Jamoos, A. Abdo and Hanna Abdel Nour, "Estimation of OFDM Time-Varying Fading Channels Based on Two-Cross-Coupled Kalman Filters," in Proc. CISSE 07, University of Bridgeport, 3–12, Dec. 2007.

[Jam11]   A. Jamoos, E. Grivel, N. Shakarneh and H. Abdel Nour, "Dual Optimal Filters for parameter Estimation of a Multivariate AR Process From Noisy Observations, " IET Signal Processing, vol. 5, no. 5, pp.471-479, August 2011.

[Kal03]   D. N. Kalofonos, M. Stojanovic and J. G. Proakis, "Performance of adaptive MC-CDMA detectors in rapidly fading Rayleigh channels," IEEE Trans. On wireless communications, vol. 2, no. 2, pp. 229-239, March 2003.

[Kal13]   Mohamad Kalil, Mohammad M. Banat and Faouzi Bader, "Three Dimensional Pilot Aided Channel Estimation for Filter Bank Multicarrier MIMO Systems with Spatial Channel Correlation," at the 8th Jordanian International Electrical and Electronic Engineering Conference (JIEEEC'2013), Aman, Jordan, April 2013.

[Kay88]   S. M. Kay. − Modern Spectral Estimation, Prentice Hall, Englewood Cliffs, NJ, 1988.

[Kev09]   Kevin Baum, Brian Classon, PhillireSartori, Principles of Broadband OFDM Cellular System Design. Wiley-Blackwell, 2009.

[Kof11]   E. Kofdisa and D. Katselisb, "Improved interference approximation method for preamble based channel estimation in FBMC/OQAM", Proc. EUSIPCO, Barcelona, Spain, 2011.

[Kof13]   E. Kofidis, D. Katselis, A. Rontogiannis, and S. Theodoridis, "Preamble-based channel estimation in OFDM/OQAM systems: A review", Signal Processing, 2013.

[Lél08]   C. Lélé, J.-P. Javaudin, R. Legouable, A. Skrzypczak, and P. Siohan, "Channel estimation methods for preamble-based OFDM/OQAM modulations," European Transactions on Telecommunications, vol. 19, no. 7, pp. 741-750, 2008.

[Lél12]   C. Lélé, "Iterative scattered-based channel estimation method for OFDM/OQAM", EURASIP Journal on Advances in Signal Processing, 2012.

[Li06]   G. Li and G. Stuber, Orthogonal frequency division multiplexing for wireless communications. Springer, 2006.

[Lin06]   L. Lin and B. Farhang-Boroujeny, "Cosine-modulated multitone for very-high-speed digital subscriber lines," EURASIP J. Applied Signal Processing, vol. 2006, 16 pages, 2006.

[Man01]   J. H.Manton, "Optimal training sequences and pilot tones for OFDM systems," IEEE Communications Letters, vol. 5, no. 4, pp. 151–153, 2001.

[Mar08]   P. Martin-Martin, R. Bregovic, A. Martin-Marcos, F. Cruz-Roldan, and T. Saramaki, "A generalized window approach for designing transmultiplexers," IEEE Trans. Circuits Syst. I, vol. 55, pp. 2696–2706, Oct. 2008.

[Mir03]   S. Mirabbasi and K. Martin, "Overlapped complex-modulated transmultiplexer filters with simplified design and superior stopbands," IEEE Trans. Signal Processing, vol. 50, pp. 456- 469, Aug. 2003.

[Ozd07]   M. K. Ozdemir and H. Arslan, "Channel estimation for wireless OFDM systems," IEEE Commun. Surveys Tuts., vol. 9, no. 2, pp. 18–48, 2007.

[San95]   S. D. Sandberg and M. A. Tzannes, "Overlapped discrete multitone modulation for high speed copper wire communications," IEEE J. Select. Areas Commun., vol. 13, pp. 1571-1585, Dec.1995.

[Sio02]   P. Siohan, C. Siclet, and N. Lacaille, "Analysis and design of OFDM/OQAM systems based on filterbank theory," IEEE Transactions on Signal Processing, vol. 50, no. 5, pp. 1170–1183, 2002.

[Sti10]   T. H. Stitz, T. Ihalainen, A. Viholainen,and M. Renforsv, "Pilot-Based Synchronization and Equalization in Filter Bank Multicarrier Communications", EURASIP Journal on Advances in Signal Processing, 2010.

[Vai93]   P. P. Vaidyanathan, *Multirate Systems and Filter Banks*, Prentice-Hall, Englewood Cliffs, NJ, USA, 1993.

[Vih09]   A. Viholainen, T. Ihalainen, T.Stitz, M.Renfors, and M.Bellanger "prototype filter design for filter bank based multicarrier transmission," 17th European Signal Processing Conference (EUSIPCO 2009).

[Wal09]   D. S. Waldhauser, L. G. Baltar, and J. A. Nossek, "Adaptive decision feedback equalization for filter bank based multicarrier systems," in Proc. IEEE ISCAS, pp. 2794-2797, 2009.

[Wan00]   Z. Wang and G. B. Giannakis, "Wireless multicarrier communications, where Fourier meets Shannon," IEEE Signal Processing Magazine, vol. 17, pp. 29-48, May 2000.

[Zha10]   H. Zhang, D. Le Ruyet, D. Roviras, "Spectral Efficiency Comparison of OFDM/FBMC for Uplink Cognitive Radio Networks," EURASIP Journal on Advances in Signal Processing, vol. 2010. doi:10.1155/2010/621808.

الموضـــوع: تقـــدير القنـــوات المضـــمحلة للنظـــام اللاســـلكي (FBMC/OQAM) باســـتخدام مرشحات Kalman

إعداد: محمود حسن خليل الدبابسة

إشراف: د. علي جاموس

الملخص

يهدف هذا البحث لحل مشكلة تقدير التغيرات في قنوات الاتصال المضمحلة للنظام اللاسلكي (FBMC/OQAM) اعتمادا على ارسال رموز استطلاعية. الحلول القياسية لهذه المشكلة هي باستخدام طرق مبنية على (LS, MMSE) مع إمكانية تطبيقها من خلال المرشحات المتأقلمة (LMS and RLS). ولكن هذه المرشحات غير مناسبة لأنها لا تأخذ بعين الاعتبار الخصائص الإحصائية لقنوات الاتصال المضمحلة. لذا، في هذه الرسالة، سيتم اختبار نوع آخر من المرشحات المثلى (dual optimal Kalman filters) التي بمقدورها اخذ الخصائص الإحصائية لقنوات الاتصال المضمحلة بعين الاعتبار من خلال استخدام نموذج الانحدار الذاتي (Autoregressive model) ليمثل قنوات الاتصال المضمحلة. ولكن هذا النموذج يحتاج إلى تعريف بعض المعاملات (parameters)، وحيث أن هذه المعاملات غير محددة القيم يجب العمل على تقديرها. وهنا تكمن أهمية الطريقة التي نستخدمها (dual optimal Kalman filters) حيث يستخدم مرشحان أحدهما لتقدير الاضمحلال في القناة والمرشح الثاني يستخدم لتقدير معاملات القناة (autoregressive parameters).

تقدير القناة المضمحلة يتم على مرحلتين: في المرحلة الأولى، حيث يتم تقدير القناة المضمحلة التابعة للرموز الاستطلاعية باستخدام المرشحات (LMS, RLS and dual Kalman filters). وفي المرحلة الثانية يتم تقدير القناة للرموز التي تعبر عن المعلومات باستخدام طرق (interpolation) منها (linear, low-pass and spline interpolations).

تم بناء نظام FBMC/OQAM باستخدام برنامج الماتلاب (Matlab) وتم تحليل النتائج، حيث تبين أن المرشح المقترح (dual Kalman filters) يعطي نتائج أفضل من المرشحات الأخرى وأن طريقة (low-pass interpolation) تعطي نتائج أفضل من الطرق الأخرى.